CALIBRATION OF CONTINUOUS VELOCITY LOGS USING THE COMPARISON OF SYNTHETIC AND FIELD RECORDS

by

BEHIC M. GURBUZ

B.Sc., University of Istanbul, 1961

A THESIS SUBMITTED IN PARTIAL FULFILMENT OF
THE REQUIREMENTS FOR THE DEGREE OF
MASTER OF SCIENCE

in the Department
of
GEOPHYSICS

We accept this thesis as conforming to the required standard

THE UNIVERSITY OF BRITISH COLUMBIA

April, 1966

In presenting this thesis in partial fulfilment of the requirements for an advanced degree at the University of British Columbia, I agree that the Library shall make it freely available for reference and study. I further agree that permission for extensive copying of this thesis for scholarly purposes may be granted by the Head of my Department or by his representatives. It is understood that copying or publication of this thesis for financial gain shall not be allowed without my written permission.

Department of Geophysics

The University of British Columbia
Vancouver 8, Canada

Date April 29, 1966.

ABSTRACT

This study is undertaken in order to calibrate the continuous velocity logs using the comparision of synthetics and field records. The results refer to the following wells in Alberta.

1. Texaco Arrowhead B-76
   60 25' 02"N, 122 59' 02" W
2. British American Morrin 7-3
   Lsd 7, Section 3, Twp 31N, Rge 20 4M
3. Cancrude British American Champion 16-29
   Lsd 16, Section 29, Twp 14, Rge 24 W 4M

The synthetic records were obtained using a linear filter model. To accomplish the synthesizing process in the laboratory, a magnetic tape function generator is used. The two-way time-depth curves are plotted for these three wells. From these curves the time intervals of continuous velocity logs were found in error by 0,007 seconds to 0,0082 seconds. The possible errors in time scale of synthetic seismograms are discussed in Chapter IV.

The comparision of synthetics with actual field seismograms recorded corresponding well locations and the main creteria for a "good match" and "poor match" are discussed.

ACKNOWLEDGMENT

Many people have provided the author with assistance and counsel during the course of this research. In particular, I wish to thank Dr. R. D. Russell for his valuable discussion and criticism of the theoretical part of this thesis. I am also indebted to Dr. R. M. Ellis for providing many helpful suggestions and for reading the manuscript critically. I would like to thank Mr. R. H. Carlyle of the British American Company Limited who provided the author with the opportunity of working on this problem with the British American Oil Company and Mr. E. F. Mahaffy of the above company for his interest and helpful assistance during the course of this research.

The study was supported in part by research grants made to Professor J. A. Jacobs by the National Research Council of Canada.

TABLE OF CONTENTS

LIST OF FIGURES

LIST OF TABLES

CHAPTER I

INTRODUCTION

1.1 Well Geophone and Continuous Velocity Surveys

The majority of well velocity surveys carried out since 1955 have used two different methods. The first method for velocity measurements is to explode charges of dynamite in a shallow drill hole alongside a deep exploratory bore hole and to record the arrival times of waves received by an in-hole detector at a number of depths which are distributed from top to bottom.

Figure 1 illustrates the setup and shows interval and average velocity curves of the type that are obtained from this procedure. The interval velocity is the distance between successive detector positions in the well, divided by the difference in arrival times at the two depths, after correction from slant path to vertical and adjusting to a datum. (Fig. 2) The average velocity is the total vertical distance divided by the total time.

1.1.1 Description and Operation of Continuous Velocity Log Sonde and Recording Devices.

The second method, continuous velocity logging, is carried out with a special type of instrument. Figure 3 shows a schematic sketch of this tool which incorporates an accoustic signal generator

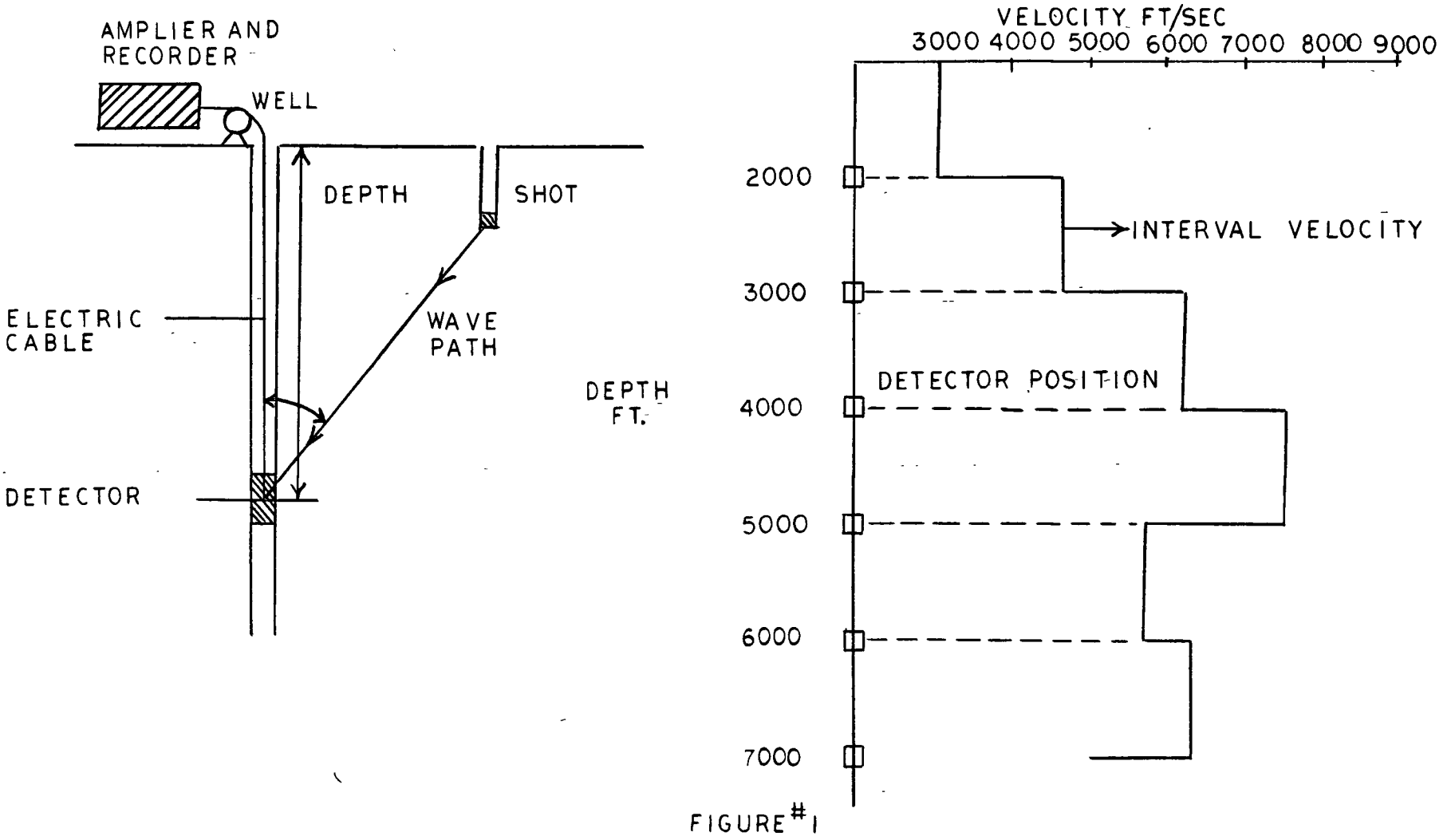

FIGURE # 1

Schematic diagram of the method by which velocity is determined by shooting in a well, and a typical interval velocity curve obtained

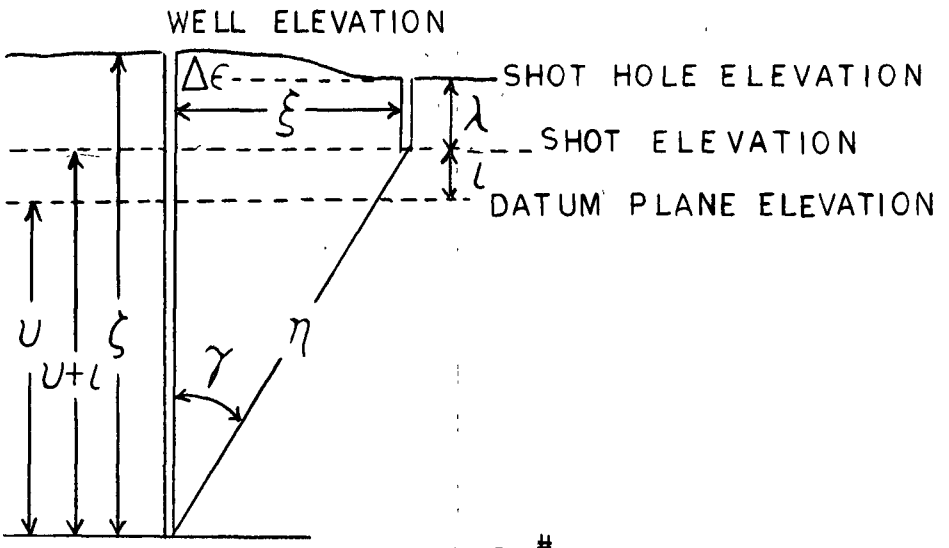

FIGURE #2

The presentation of results of well shooting

U = Geophone depth measured from datum elevation.

ι = Difference in elevation between shot and datum plane.

$U+\iota$ = Geophone depth measured from shot elevation.

ζ = Geophone depth measured from well elevation.

η = Straight line travel path from shot to well geophone.

ξ = Horizontal distance from well to shot point.

λ = Depth of shot.

t_s = Uphole time at shot or other surface reference time.

$t_e = \frac{\iota}{V_e}$ = Vertical time from shot to datum plane.

T = Observed time from shot to well geophone.

$U+\iota = \zeta - \lambda - \Delta\epsilon$

$\Delta\epsilon$ = Difference in elevation between well and shot point.

$T_c = \overline{T} - t_e$ = Vert. travel time from datum plane to geophone.

$\overline{T} = \cos\gamma\, T$ = Vert. travel time from shot elevation to geophone.

V_a = Average velocity = $\frac{U}{T_C}$

V_i = Interval velocity = $\frac{\Delta U}{\Delta T_C}$

V_e = Topmost velocity in consolidated layer.

U = d - (Kelly Bushing elevation - Elevation Datum).

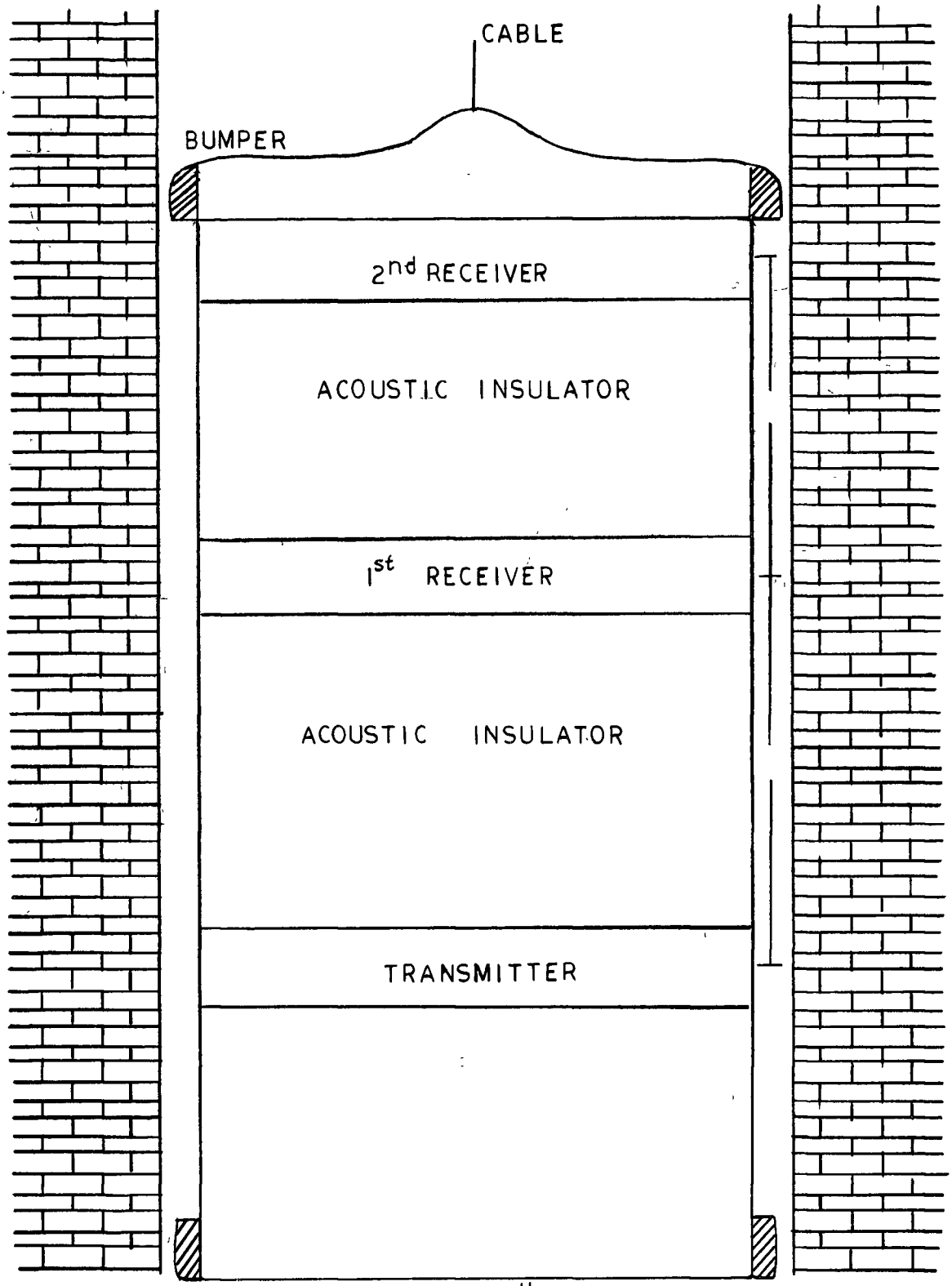

FIGURE #3

Schematic diagram of 4'X5' continuous velocity tool.

(transmitter) which emits pulses that travel through the formation side walls to the receivers. The transmitters and receivers are spaced vertically about 5 feet apart and are insulated from each other by acoustic insulation. The distance between the transmitter and the first receiver must be large enough so that the first signal to reach this receiver travels through at least a small part of the formation which is to be measured. This condition obviously cannot be satisfied in formations in which the velocities are slower than in the mud. When formation velocity exceeds mud velocity, the minimum required spacing between transmitter and the first receiver is proportional to the stand-off (i.e. the seperation between the wall of the hole and the tranducers) and is a function of the ratio of mud velocity to formation velocity. The relationship may be derived by straightforward computation of the total time for an acoustic pulse to travel from transmitter to receiver. The result is

$$\frac{d_{min}}{S} = 2\sqrt{\frac{1+\alpha}{1-\alpha}}$$

where

d_{min} = minimum required distance between transmitter and receiver

S = stand-off

α = ratio of mud velocity to formation velocity.

The first arrivals of the acoustic signals at the two receivers are recorded directly on the film. Figure 4 is simplified

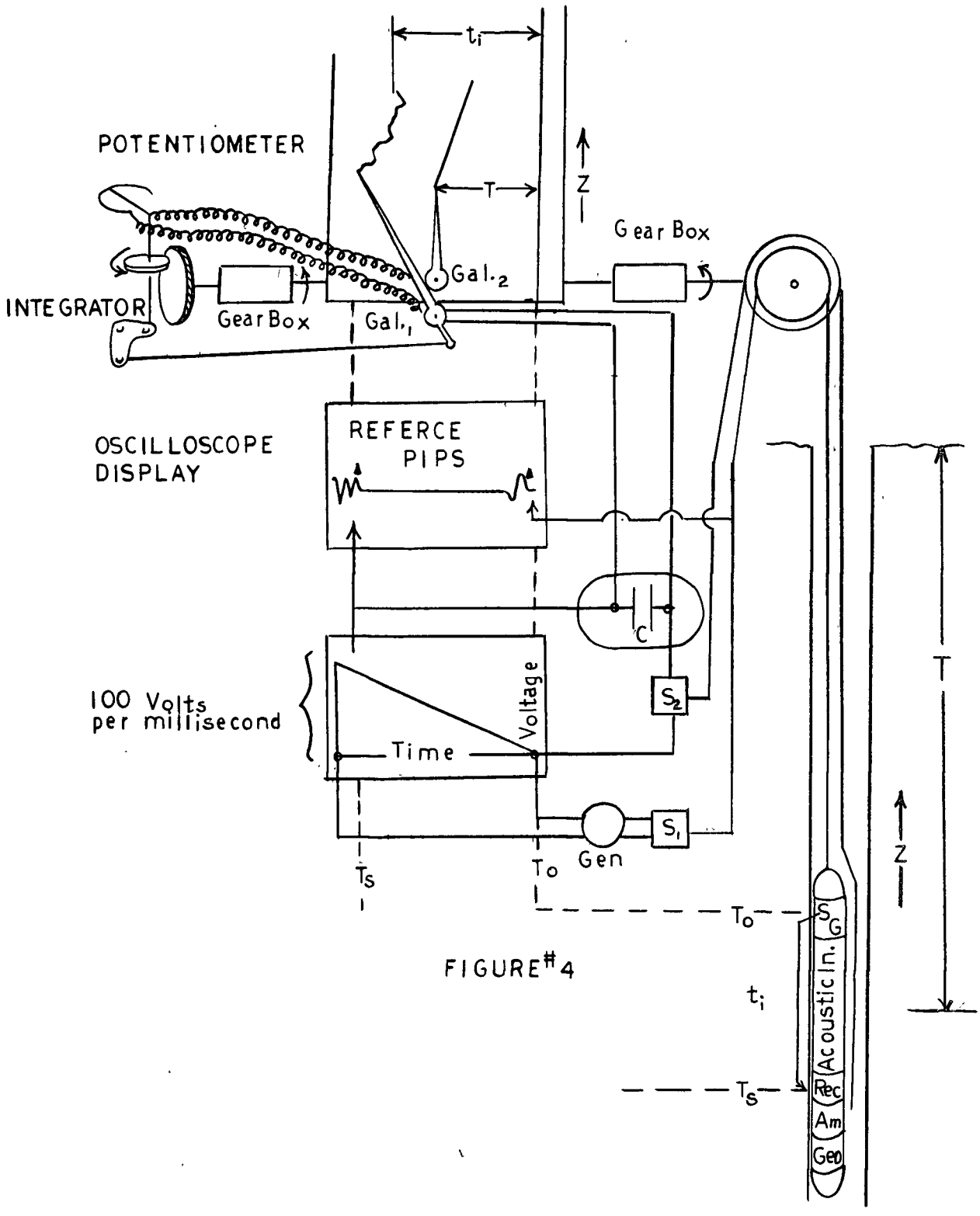

FIGURE #4

Diagram of continuous velocity logger.

diagram of the continuous velocity logger for the single receiver pulse system. At the pulse instant, switch S_1 closes, starting the sawtooth generator Gen, which develops a voltage proportional to time.

When the acoustic signals arrives at receiver Rec_1, switch S_2 is closed discharging the generator voltage, as of that instant, into condenser C. This voltage is impressed on galvanometer Gal_1 the pointer of which traces the value of t_1 on the log at the indicated depth.

The time-instant of the signal and its arrival at receiver Rec are displaced on an oscilloscope.

The integrator provides the over-all travel time T for the interval logged by continuous integration of the t_1 curve.

The continuous velocity logs then consist of two curves:

(a) The interval velocity curve. This curve is the continuous recording of the interval time in microseconds through individual formations along the entire vertical extent of the well, and can be read as interval velocity on the appropriate scale at the top of the log.

(b) The integrated curve. This curve is derived by direct summation of the interval velocity curve, and is calibrated to the geophone surveys. Total travel times over any section of the log may be obtained from it.

The results of time determinations surveyed by both methods do not agree and discrepancies up to several tenths of milliseconds for deep wells occur. The usual procedure is to survey a well with both methods. When the survey is interpreted, the continuous velocity data adjusted to the well geophone survey. The usual argument for this procedure is that the well geophone survey simulates more closely the conditions encountered in seismic shooting. The interval velocity curve is therefore laterally displaced, and the slope of the integrated curve is adjusted before final drafting, using a corrected time.

The reflection horizons are not always obvious from a continuous velocity log. They reflect the lithology and are often very similar to resistivity logs. The reflection horizons versus velocity contrasts can be correlated from well to well in a given area.

1.1.2 The Observed Time Discrepancies Between Continuous and Velocity Surveys. The results of the statistical analysis of the observed time discrepancies between continuous and velocity surveys showed that there is both a normal random discrepancy and a systematic deviation between the observed time of the velocity and the well geophone surveys (Gretener 1963). It is found that certain important factors strongly influence the deviation found between the two types of surveys.

The study of continuous velocity surveys is subject

to three sources of errors. First of all a problem arises in the presence of non ideal tool geometry. Laboratory studies and surveys in wells (Hicks 1959, Kokesk and Plizard 1959, Wyllie, Gregory and Gardener 1958), showed that in the invaded (penetrated by drilling fluid) zone around a well, the apparent velocity is lower than in the virgin formation. The major factors effecting the thickness of the low velocity zone are the consolidation, porosity, and mineral composition of the formation being penetrated. The continuous velocity measurements acquire the character of refraction surveys and unless the spacing (distance between receiver and transmitter) is sufficiently large (Fig. 3), the first arrivals will not have travelled through the virgin formation. It is thus desirable to extend the spacing to the maximum possible length.

A further potential source of error arises from the problem of the improper centering of the tool in the hole. The tool is equipped with removable rubber bumpers and centralizers of approximately 5 inches in diameter. With the high logging speeds, the flow of mud around the tool will also tend to keep the tool centralized. Therefore, a systematic deviation due to a constant inclination of the tool in the hole, seems improbable.

It is further found that the results may be affected by possible wave dispersion in the frequency range 50-12,000 c.p.s. We have little available information concerning wave dispersion. Birch and Bancroft (1958) have investigated this

phenomenon in granite in the range 140 to 4,500 c.p.s. They have measured the flexural, torsional and longitudinal modes. The first two modes do not indicate any increase in velocity, while the last one shows an increase in velocity of about 0.5% over the range 850 to 4,300 c.p.s., which lies well within the limit of error. They have concluded that for these frequencies, the velocities were independent of frequency to within 1% or less.

Bruckshaw and Mahanta (1952) have also studied this problem in the range of 40 to 120 c.p.s. for various rock types such as diorite, dolerite, limestone and sandstone. The velocity-frequency curves of these rocks are quite similar, showing an increase of the wave velocity with frequency of about 1.5% in the range of 40 to 120 c.p.s. These curves indicate that the rate of increase diminishes with higher frequencies.

One can conclude that there is evidence that the wave velocity increases slightly with frequency.

Although there are two major sources of errors in the well geophone surveys, it is also found that there are many possible effects which could cause a degree of randomness in the observed data. The most important single source of error is the delay of the signal due to the changing electrical properties of the setup during the survey. For shallow shots, an unshielded well geophone cable having a high inductance and low capacitance is wound on the drum while for deep check

shots the capacitance is high and inductance is low. This, of course, might introduce a lag into the well geophone survey. An attempt has been made to eliminate this possibility. An experiment was set up whereby a pulse was recorded directly and also after going through the cable and the downhole geophone. The results of this experiment have not shown any delay. However, it has been noticed that in the case of poor breaks, some kind of later event might be picked rather than the true first arrivals.

Studies at different locations indicated that anisotrophy is indeed a rather common phenomenon. In a simple case of anisotropy, the velocity parallel to the surface will be greater than that at right angles to it. If the beds are undistributed, the horizontal velocity is greater than the vertical velocity in the medium above the geophone level. The anisotropy factor may be given by the ratio of the horizontal velocity to the vertical velocity.

In any intermediate direction the velocity has a value V_B, whereby $V_h \rangle V_B \rangle V_Z$. Figure 5 shows the affect of anisotropy in the shallow layers on a well geophone velocity survey. For the very shallow check-shot levels, the angle is large and the ray travels at a velocity V, which is about $(V_h + V_Z)/2$, while for the deep levels the angle becomes small and the ray travels through the same shallow layers at a velocity very close to V_Z.

Consequently, an error is committed when correcting the shallow check-shot times to vertical time by a mere

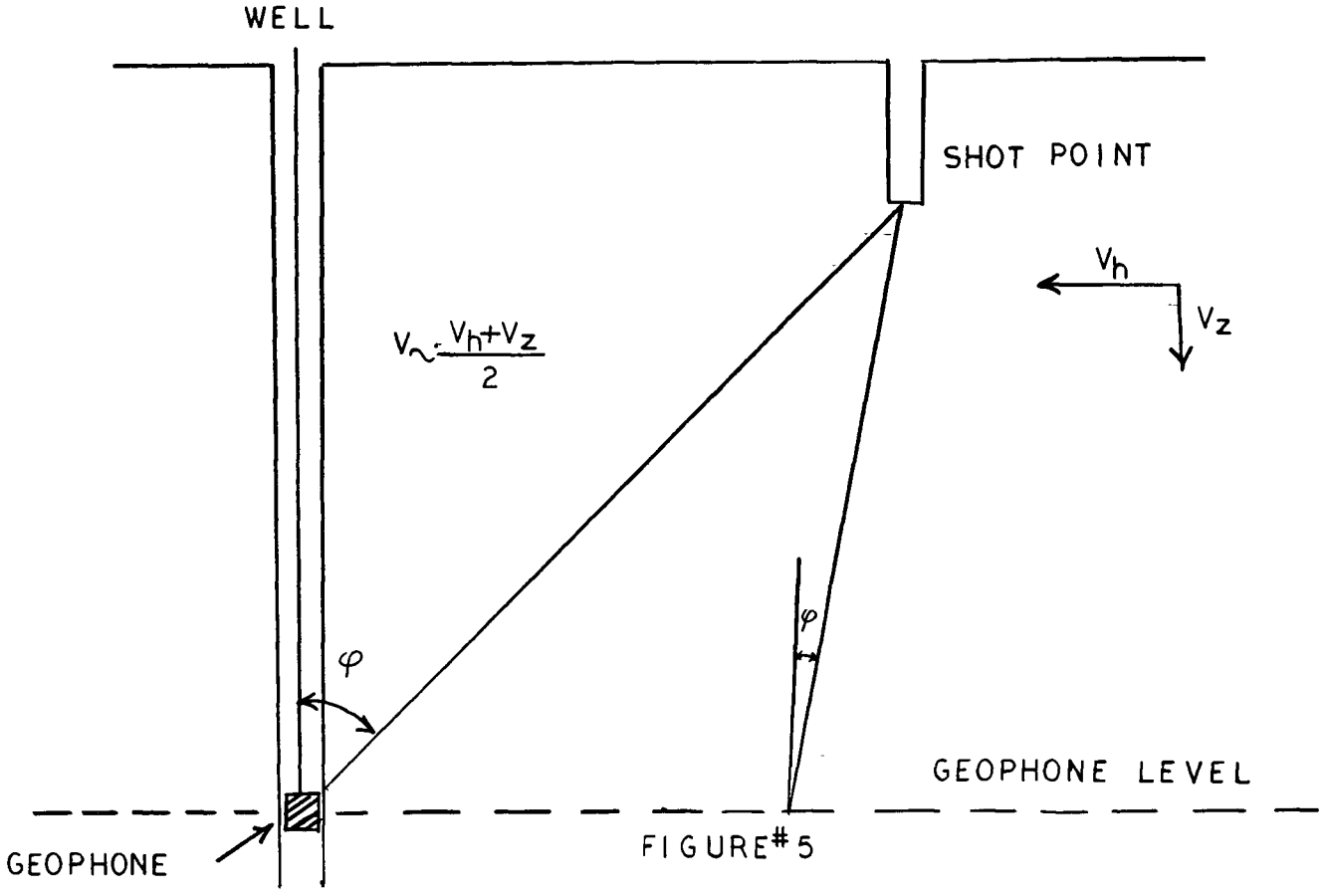

Effect of anisotropy on conventional well velocity survey

multiplication with cos φ . The times for the shallow check-shot levels will be short if no allowance is made for anisotropy, while the times for the deep levels will be correct. For anisotropy factor of 1.1 and various velocities the error is zero at the surface and increases to a maximum for signals arriving at 45 degrees.

It should be taken into consideration that a curvature in the raypath will cause the same type of error. If we do not have available continuous velocity data from the surface downwards, it will in most cases be impossible to determine whether such an error is due to true anisotropy, or curvature of the raypath or combination of both.

1.2 The Synthesis of Seismograms from Continuous Velocity Log Data.

Recent developments of continuous velocity log surveying and its logging devices and acquisition of substantial amounts of data have materially increased the potentialities of such investigations. Under simplified but realistic physical assumptions, the basic data from continuous velocity surveys in wells can be used to simulate the variations in acoustic impedance in the ground which gives rise to seismic reflections. This argument has been put forward by Peterson et al. (1954), who they describe an analogue computer which makes use of the basic well data to procedure synthetic seismic records resembling actual field seismograms. To accomplish this synthesizing process in the laboratory magnetic tape function generator is being used (Fig. 6).

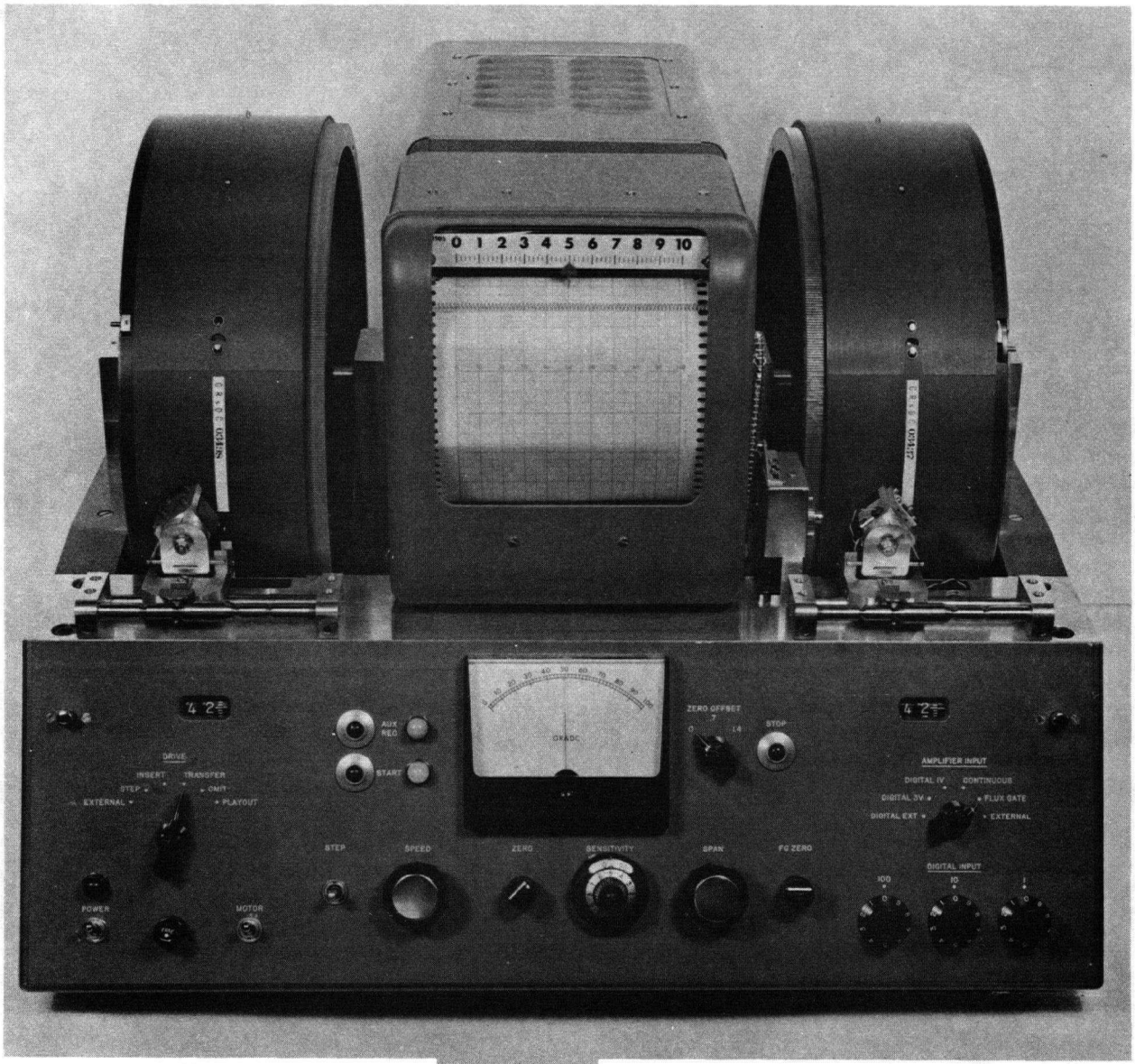

FIGURE #6

Front view of magnetic tape function generator

Correspondance between the synthesized record and actual seismic record made over the well is quite good in many cases, even though some of the conditions which occur in nature (noise, multiple reflections, for example) are not simulated in the synthesis. The technique is particularly useful for showing the effect of small changes in velocity or layer thickness upon the wave form of a reflection. More recent studies have been made Berryman (1958) and Wuenschel (1960) who have described models which contain all multiples. Backus (1959) introduced water reverbations into the model. Lindsey (1960) introduced ghosts in the same way that Backus introduced reverbations.

Up to this point, we have briefly outlined the process of two well velocity survey methods and have discussed possible causes for time discrepancies between continuous velocity and well geophone surveys and the calibration of continuous velocity logs according to the well geophone data. Finally, we have mentioned the sythesis of seismograms.

In our studies, we have attempted to calibrate continuous velocity logs using comparisions of synthetics and field records rather than well geophone survey.

CHAPTER II

THEORY

2.1 Theory of the Linear Filter Model of Peterson and his Co-Workers.

In the use of this model several assumptions are made in order to make the problem tractable. The model earth is assumed to be transversly isotropic, and is characterized in the vertical direction by continuous velocity function $v(z)$, that is obtained from a continuous velocity log. The density function $\rho(z)$ of the model is related by any general expression of the form

$$\rho(z) = k\left[V(z)\right]^{m} \qquad (1)$$

where k and m are constants.

The shot pulse propagates in the vertical direction as a plane wave, thus striking the layers at normal incidence and reflections result exclusively from velocity changes due to the assumed relationship between density and velocity. Furthermore only primary reflections are included, all types of "noise" such as ground roll, multiples and ghosts are excluded. The shot pulse wave form is time-invariant (the properties of the filter are independent of time) its shape and amplitude are constant and do not change with travel time.

One generally accepted standard method of filter

characterization is its impulse response. (Fig. 7.) An input impulse of unit area will procedure a characteristic transient output waveform $u(t)$. There are two restrictions of the function $u(t)$ in any physically realizable filter:

$$u(t)=0 \quad \text{for} \quad t<0$$
$$u(t)\to 0 \quad \text{for} \quad t\to\infty \tag{2}$$

An arbitary input $f(t)$ will be modified in passing through the filter and give an output which will be a function of both $f(t)$ and $u(t)$. The mathematical expression of this output will be given by convolving $f(t)$ with $u(t)$. The mathematical operation of convulation is designated by a star, and is defined by the following relationship:

$$S(t)=f(t)*u(t)=\int_0^t f(t)\,u(t-\tau)\,d\tau \tag{3}$$

Figure 8 shows a single interface separating two semi-infinite media. The velocity above the interface is v_1 and the velocity below is v_2. The densities above and below the interface ρ_1 and ρ_2. The density-velocity product between two rock layers will be $\rho_1 v_1$ and $\rho_2 v_2$. The pulse propagates downward as a plane wave with normal incidence interfaces. The reflection coefficient is defined as the ratio of the reflected wave amplitude to the incident wave amplitude. It is equal to

$$R=\frac{\rho_2 V_2-\rho_1 V_1}{\rho_2 V_2+\rho_1 V_1} \tag{4}$$

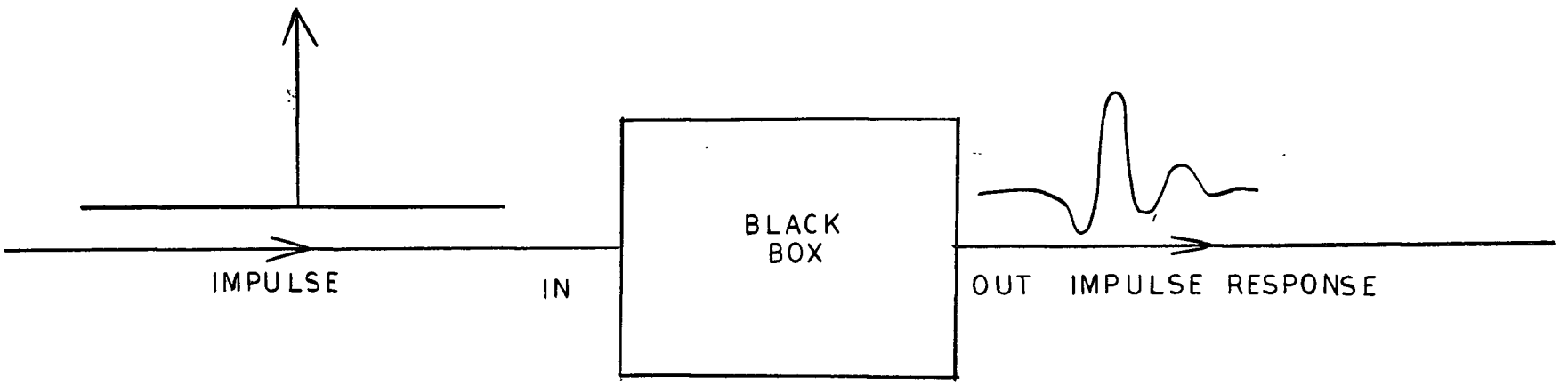

FIGURE#7

Impulse response of a linear filter

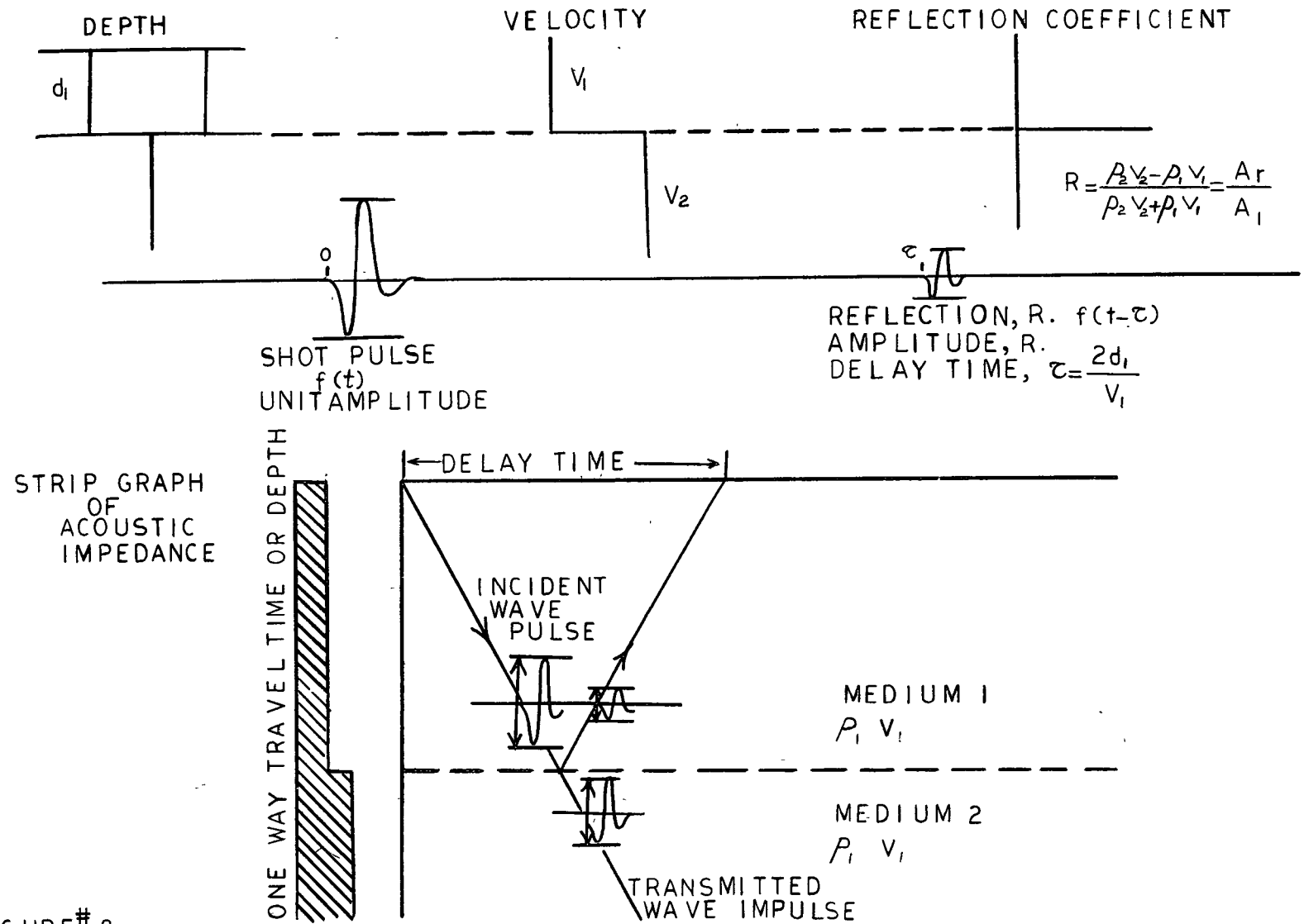

FIGURE# 8

Schematic illustration of the reflection process for two acoustic interfaces

assuming the density to be constant, we can write this relationship as follows:

$$R = \frac{V_2 - V_1}{V_2 + V_1} \qquad (5)$$

As was mentioned in the discussion of the properties of this model, the density (ρ) is assumed constant or proportional to some power of the velocity. The reflected pulse has identically the same shape and breadth as the incident pulse, but differs in amplitude. When the incident wave propagates from a medium of low velocity, the reflection coefficient is positive and its polarity will be the same as the shot pulse. On the other hand, when the incident wave travels from a medium of high velocity into one of lower velocity, the corresponding reflection coefficient is negative and its polarity will be reversed. The beginning of the reflection occurs at the time τ, which is the two-way travel time to the interface. Thus, if one designs the shot pulse $f(t)$, the reflection can be written $R_1 f(t-\tau)$. This model can be extended to velocity interfaces occurring at infinitisimally small depth intervals (Fig. 9). Each reflection has its own polarity, amplitude and time delay, but has the same wave form as the time-invariant shot pulse. The sum of all the reflections will be the output of this model.

$$S(t) = R_1 f(t-\tau_1) + R_2 f(t-\tau_2) + \cdots \qquad (6)$$

if written as a summation:

$$S(t) = \sum_{i=1}^{n} R_i(\tau_i)\, F(t-\tau_i) \qquad (7)$$

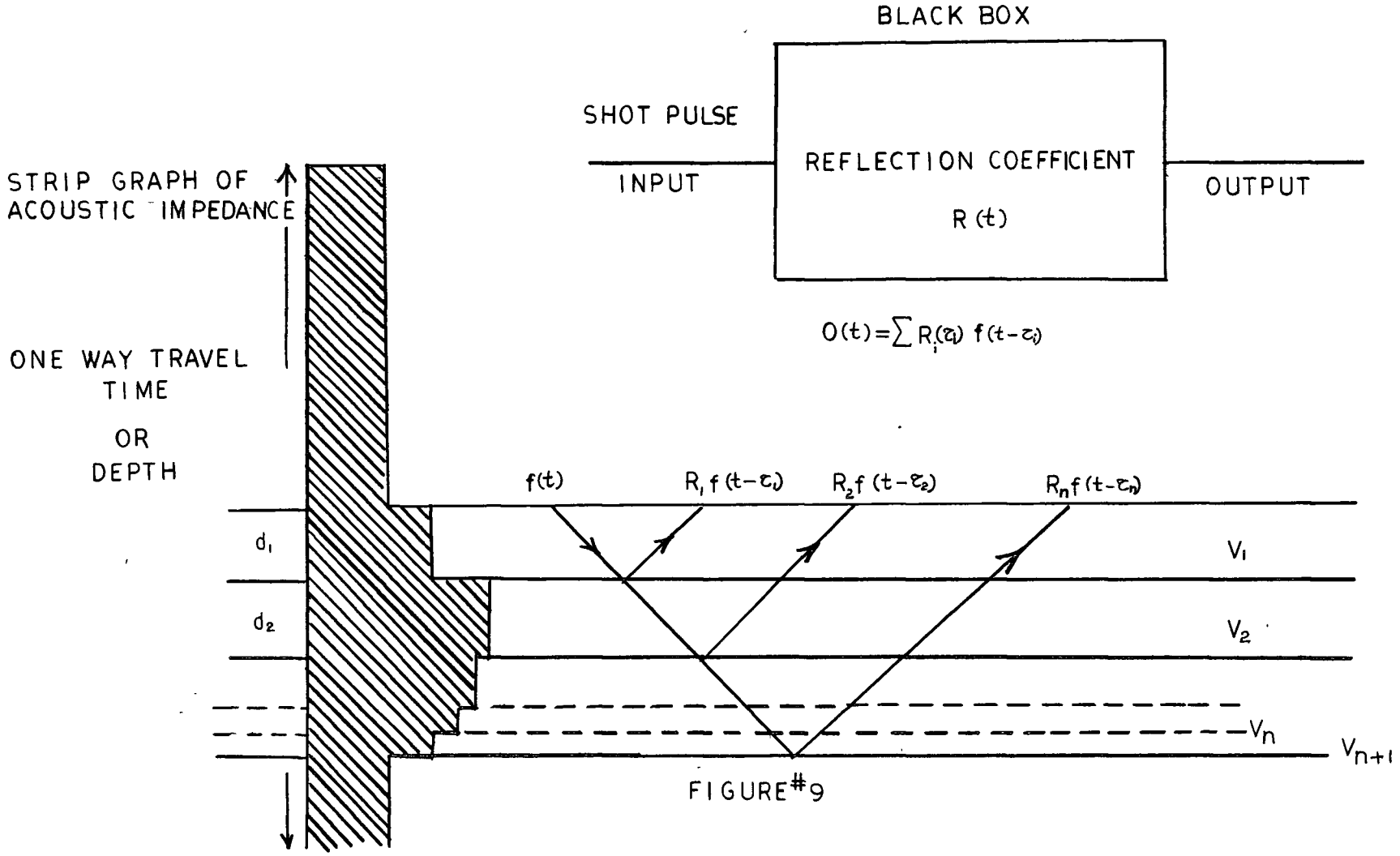

FIGURE #9

Schematic illustration of the reflection process with 'n' interfaces

The equation (7) describes the reflection process in the "n" layered model. This equation shows that the reflection process of Peterson's model is a linear filter process. The earth can be assumed as a filter which impulse response is the set of reflection coefficients spaced suitably in time. The model can be extended from "n" layers to a continuous velocity distribution as the layer thickness approaches zero. Then equation (7) becomes convolution integral.

The continuous velocity log gives the complicated layering of the earth, and it can be sampled to give a many layered model. The reflection coefficients can be calculated using equation (5). Peterson introduced a simplification by using an approximate expression for the reflection coefficients. In equation (5), v_2 can be written as $\rho v_1 + \Delta(\rho v)$. Then equation (5) becomes:

$$R_1 = \frac{[\rho V_1 + \Delta(\rho V)] - \rho V_1}{[\rho V_1 + \Delta(\rho V)] + \rho V_1} \tag{8}$$

$$R_1 = \frac{\Delta(\rho V)}{2\rho V_1 + \Delta(\rho V)} \tag{9}$$

If a continuous velocity log is sampled at sufficiently small intervals, the equation (9) can be written as follows:

$$R_1 \cong \frac{1}{2} \frac{\Delta(\rho V)}{\rho V_1} \tag{10}$$

or,

$$R \cong \frac{1}{2} \Delta \log(\rho V) \tag{11}$$

This approximation gives reasonable results for reflection coefficients less than $\pm$ 0.4. In this model, the density is considered constant, so that the above relationship (11) can be further simplified to give:

$$R \cong \left(\frac{1}{2} \Delta \log V_1 \right) \tag{12}$$

This expression states that the amplitude of the wave reflected by each incremental change or "step" in acoustic impedance is proportional to the corresponding incremental change in the value of the logarith of acoustic impedance.

In relationship (1) if k and m are constants, the acoustic impedance can be expressed as follows:

$$\rho V = k V^{m+1} \tag{13}$$

When substituting the above value in equation (11), the reflection coefficient becomes:

$$R \cong \frac{1}{2} \Delta \log k V^{m+1} \tag{14}$$

This can also be written as follows:

$$R \approx \frac{1}{2} \left[\Delta \log k + (m+1) \Delta \log V \right] \tag{15}$$

since k is a constant, the equation (15) can be written in the form.

$$R \approx \frac{m+1}{2} \Delta \log V \tag{16}$$

In the above expression (16) the reflection coefficient is also proportional to the change in the logarithm of velocity

The continuous velocity log shows the velocity distribution with respect to depth. This is converted to velocity as a function of two-way travel time. In the discrete layer case, the reflection amplitude is determined by the reflection coefficients, using equation (5) or approximation (11). Otherwise the continuous set of reflection coefficients is replaced by the reflectivity function $r(t)$. The reflectivity function can be made more useful in relationship (9) by letting Δt approach zero as a limit. This can be done by following the steps as shown below:

$$\lim_{\Delta t \to 0} \frac{R'}{\Delta t} = \lim_{\Delta t \to 0} \frac{\Delta V}{\Delta t} \frac{1}{2V + \left(\frac{\Delta V}{\Delta t}\right)\Delta t} \tag{17}$$

$$= \frac{1}{2V}\left(\frac{dV}{dt}\right) \tag{18a}$$

$$= \frac{1}{2V} \frac{d}{dt}\left[\text{Log } V(t)\right] \tag{18b}$$

The constant 1/2 on the right side of this equation is merely a gain factor and it can be ignored. The logarithm of velocity as a function of time is called the velocity function. Then the first derivative of the velocity function with respect to time is defined as the reflectivity function:

$$r \triangleq \frac{d \text{ Log } V(t)}{dt} \tag{19}$$

2.2 To Convert a Continuous Velocity Log to the Reflectivity Function

Figure (10) is a block diagram which shows how to convert a continuous velocity log to the reflectivity function. Since the reflection process is a filter process, there are two alternate ways to accomplish the filtering process in Peterson's model (Figure 11). The first normal way for the reflection process is to consider the shot pulse as the input and the reflectivity function as the impulse response of the filter. As it has been mentioned in the previous discussions, the mathematical theory of this model is dependent upon convolution. We know that the convolution has commutative operation, (i.e. $f(t) * g(t) = g(t) * f(t)$) therefore, the input and the filter can be interchanged, using the reflectivity function as an input and the shot pulse as the impulse resonse of the filter. This is Peterson's analogue method of preparing synthetic seismograms. The filter settings that act upon the reflectivity function have been divided into two parts, namely the shot pulse and the filtering external to the earth. The latter includes the combined effect of all instruments plus geophone coupling (Figure 11).

2.3 Comparison of Synthetic and Actual Field Seismograms

Before attempting to approach our problem, we have studied the comparison of synthetics with actual field seismograms recorded at corresponding well locations. Fig. 12 shows the area studied.

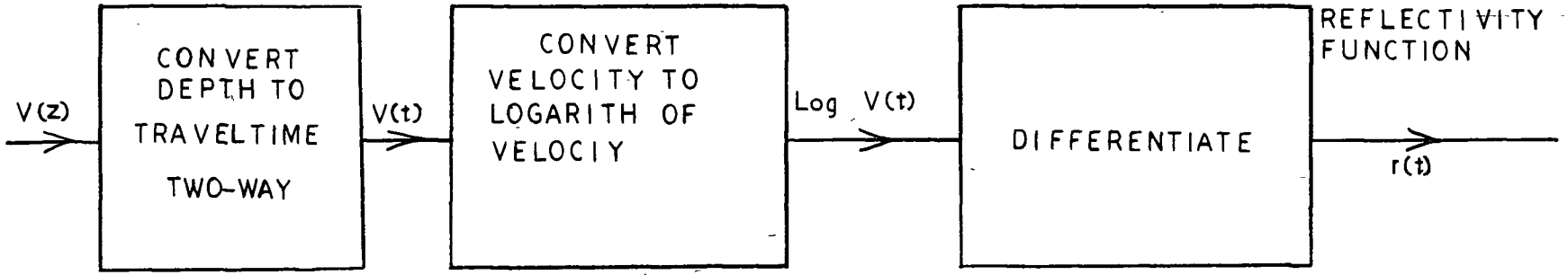

$$r(t) \triangleq \frac{d}{dt} \log v(t)$$

FIGURE # 10

Block diagram of the convertion of a velocity log to the reflectivity function

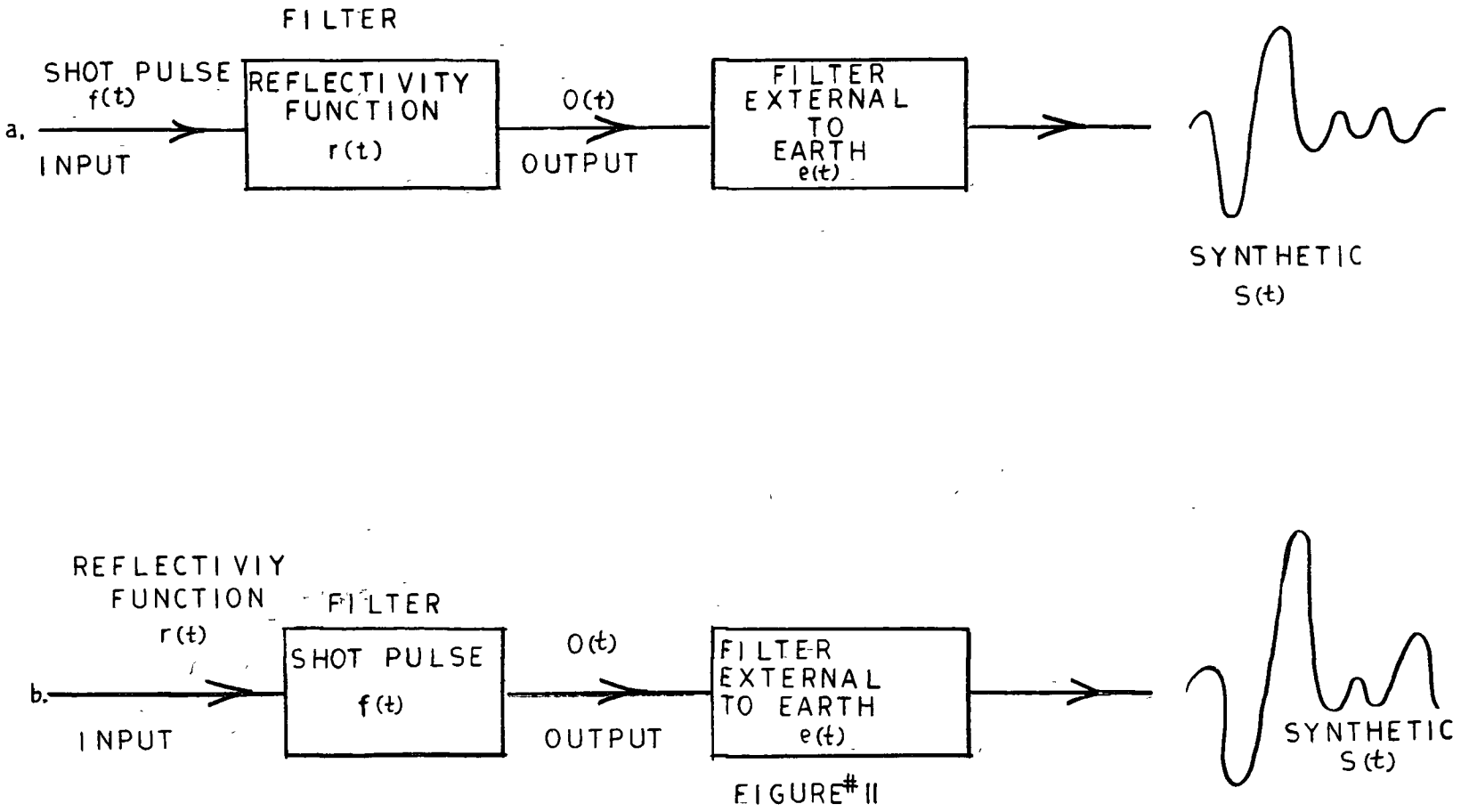

FIGURE# II

Two alternative ways of representing the reflection process in a linear filter

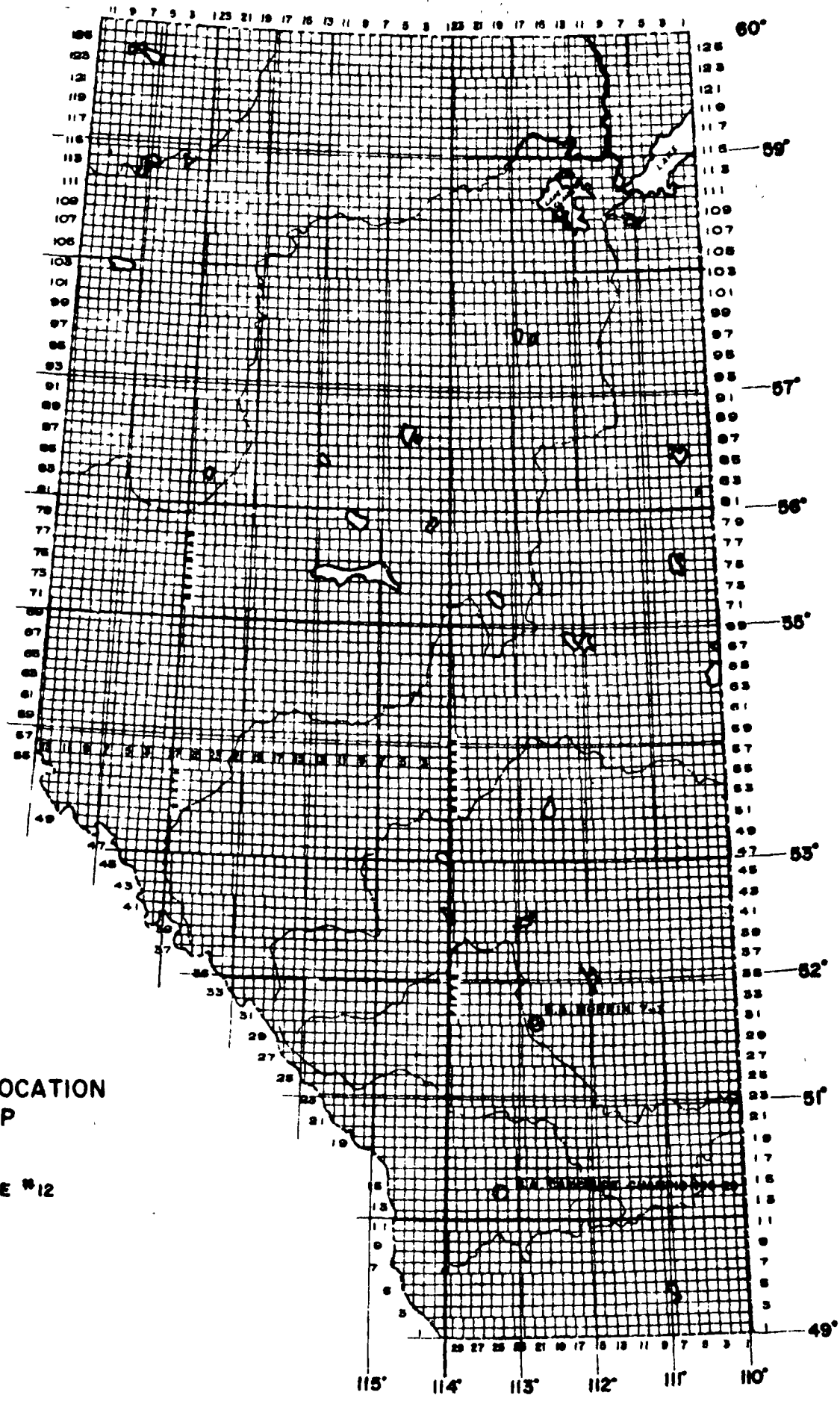

WELL LOCATION MAP

FIGURE #12

As a result of these studies, reasonable correlations were obtained at thirteen different locations, while a few locations showed "poor" matches.

There are three main criteria for a good match.

1. The synthetic and actual field record should match in character. Both records should have the same interval time between large reflection events and have also the same "dead" zones.
2. When the field and synthetic records have the best character match, they should also have the same filter delay.
3. The polarities of both records should be consistent. If the polarity of the field record is established by making the initial signal break-down, a step velocity change in the earth from low to high velocity will result in a reflection that initially breaks down on the actual field record. The polarity of the synthetic record can be set to the polarity of the field record by placing an isolated step on the velocity function and observing the initial break of its reflection.

In general, there are three possible reasons for a poor match in comparison with the synthetic and actual field records.

1. The filtering on the synthetic may not duplicate the filtering on the actual field record. It should be taken into account that the actual field record contains a shot pulse filter as well as all filtering external to

the earth such as, geophone coupling, amplifier filter, geophone response, (Automatic Gain Control) and so on.

2. The original continuous velocity log is subject to error in some of the formations. The most important ones are due to washouts in salt and shale formations.
3. The assumption made in the theory of this model may not hold sufficiently well in the actual earth. The primary poor assumption is that the record only includes primary reflections. All types of noise such as ground roll, multiples and ghosts are excluded.

The second poor assumption is that the density as constant or proportional to velocity. This assumption is poor in some formations such as salt and anhydrite.

2.4 Multiple and Ghost Reflections:

Based on experience and physical reasoning, conditions conducive to the formation of multiple reflections are:

(a) the existance of strata which reflects a large percentage of the incident energy or formations having minumum attenuation and absorption of seismic energy by secondary effects (diffraction, diffusion etc.).

(b) surface conditions such that explosive charges are efficient and a large percentage of the emergent energy is reflected from the ground surface.

The significance of multiples to the total reflected signal depends on the vertical distribution of acoustic impedance. For small contrasts in acoustic impedance, multiples

can produce discrete events, cause phase shifts in large amplitude, direct reflections, and alter the frequency of weak, direct, reflected signals. If the near surface contrasts are large, then multiples within these layers can mask a direct reflected signal from depth by producing "ringing" or "wave training". Multiples cause distortions. The magnitude of distortion cannot be observed on the seismograms.

The existance of a large velocity discontinuity above a seismic shot can be recognized as the source of "ghost" reflections appearing on the seismogram. In such instances, the downgoing wave front set up by the shot is characterized by energy moving directly downward from the shot point followed in space and time by energy reflected from the overlying discontinuity. When detected this downgoing wave front appears as two wavelets displaced in time by approximately twice the travel time from the shot to the discontinuity and with possible differences in shape. Any difference in shape may be attributed to resonance effects of the ground between the shot and the discontinuity and the sphericity of the incident wave front at the discontinuity. Recent studies have made possible the eliminating of the ghost reflections on magnetically recorded seismograms by means of a linear filter. This additional filter includes both the velocity layering above the shot and the additional attenuation in the ghost path. The application of this filter does not alter significantly the character of primary reflections although eliminating the ghost reflections.

CHAPTER III

CALIBRATION OF CONTINUOUS VELOCITY LOGS USING COMPARISON OF SYNTHETIC AND FIELD RECORDS RATHER THAN WELL GEOPHONE SURVEY DATA

3.1 Procedure

The writer has attempted to calibrate continuous velocity logs by comparing synthetics and field records as follows:

1. First, the function generator tapes and their playouts are made from the uncalibrated continuous velocity logs following the same three steps which are shown in Figure 10.
2. The filtering used in making synthetics is generally determined empirically, using two band pass filters - one matching the filter used on the field record (instrument filter) and the other simulating the filtering action of the shot pulse (earth filter). The instrument filter is known (obtained from actual field data), therefore, the second filter is varied to give the best character match between actual field and sythetic records. This can be done by changing the low and high cut-off frequency ranges of the earth filter until the best correlation between them is obtained.
3. The time intervals are set on both records at every 100 milliseconds. The time intervals should be set on the field record after making the time correction for weathering and elevation variations (Figures 13,

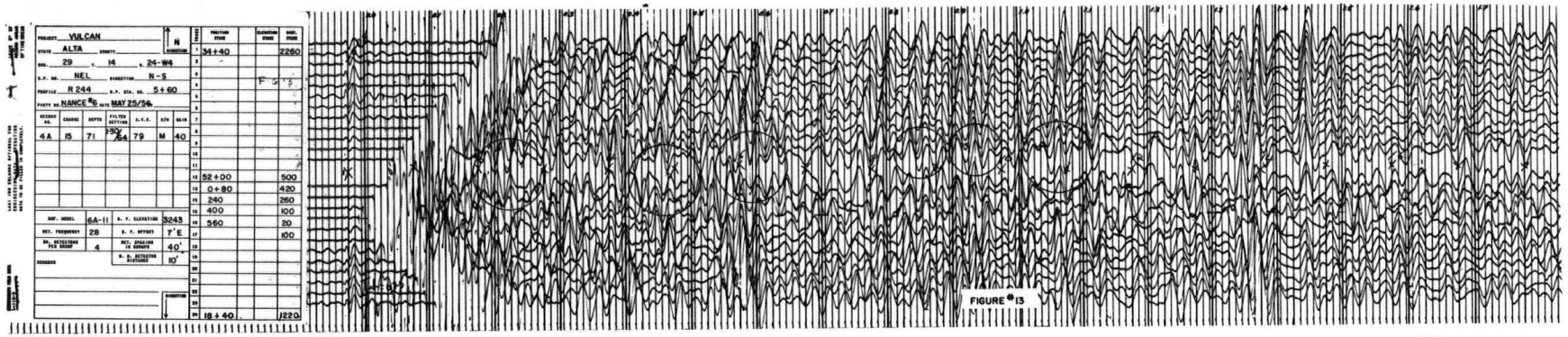

B.A. Cancrude Champion 16-29 field record

B.A. Morrin 7-3 field record

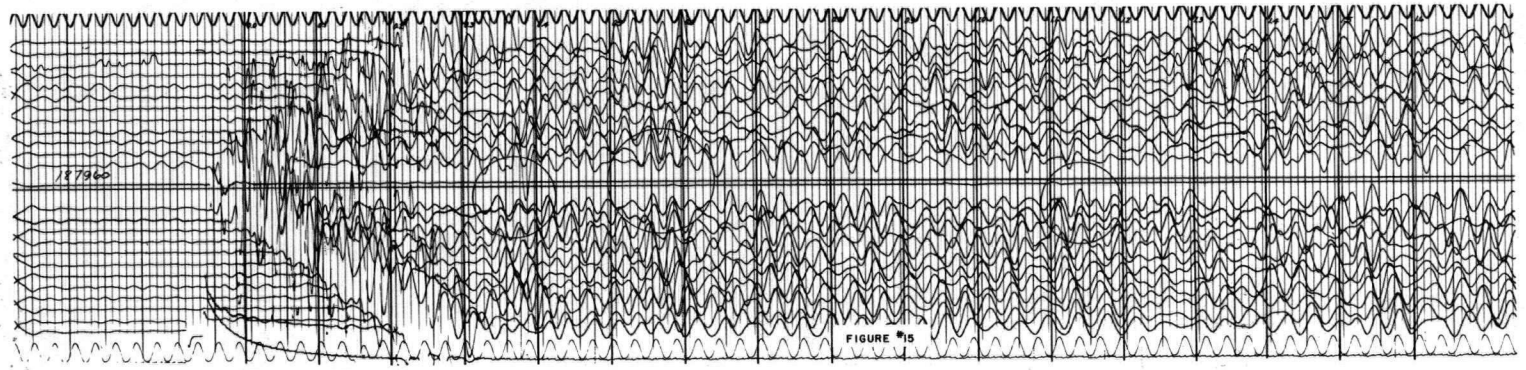

B.A. Texaco Arrowhead B-76 field record

14, 15). When making this correction, the elevation datum of the well data should be used. It is arbitrarily assumed that the starting point of the synthetic trace is zero time. As it can be seen, there are two traces on the synthetic playback record (Figures 16, 17, 18). The upper one is the synthetic trace. The lower one shows the velocity function. If one considers the correspondence between the velocity function and the synthetic trace, it is not surprising that the resulting synthetic trace will have similar character, but will be later in time. This is simply a filter delay. The amount of this filter delay is related to the impulse response wave form, which, in the case of the synthetic seismogram is given by the reflection from a step velocity function. Therefore, the zero time interval is set on the starting point of the synthetic trace, not on the starting point of the velocity function, because the correlation results of the synthetic and field record time intervals will be used and not the correlation between the velocity function and field record.

4. In this step, the synthetic and actual field records are correlated. The correlation can be made between apparent reflection peaks (Figures 19, 20, 21). It is known that when the field and synthetic records show the best character match, there should be no relative time-shift between them. Therefore, if one obtains

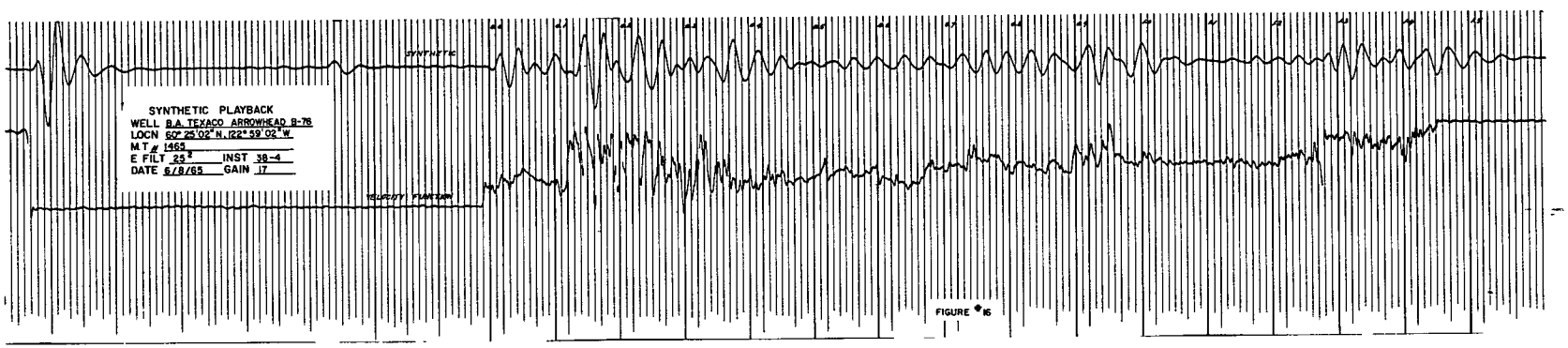

B.A. Texaco Arrowhead B-76 synthetic playback

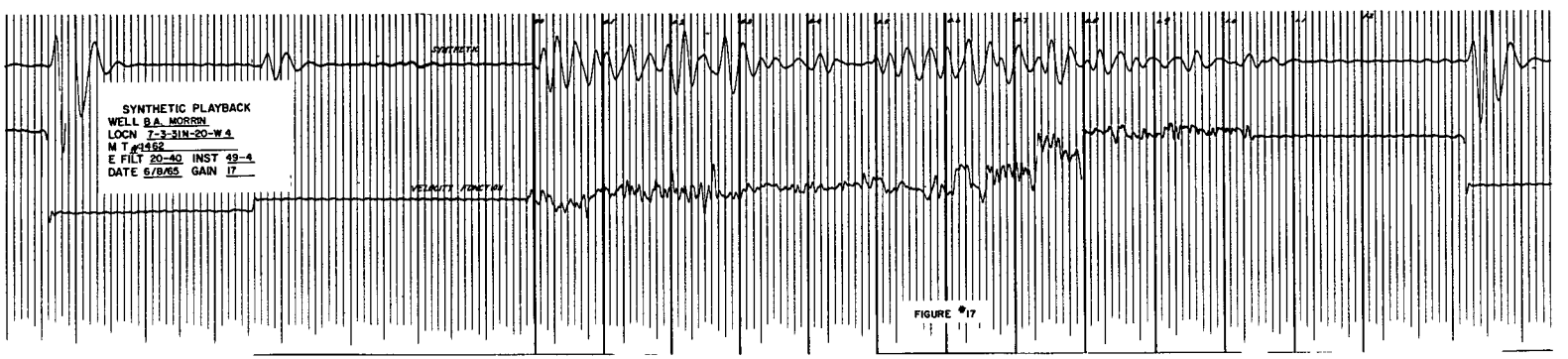

B.A. Morrin 7-3 synthetic playback

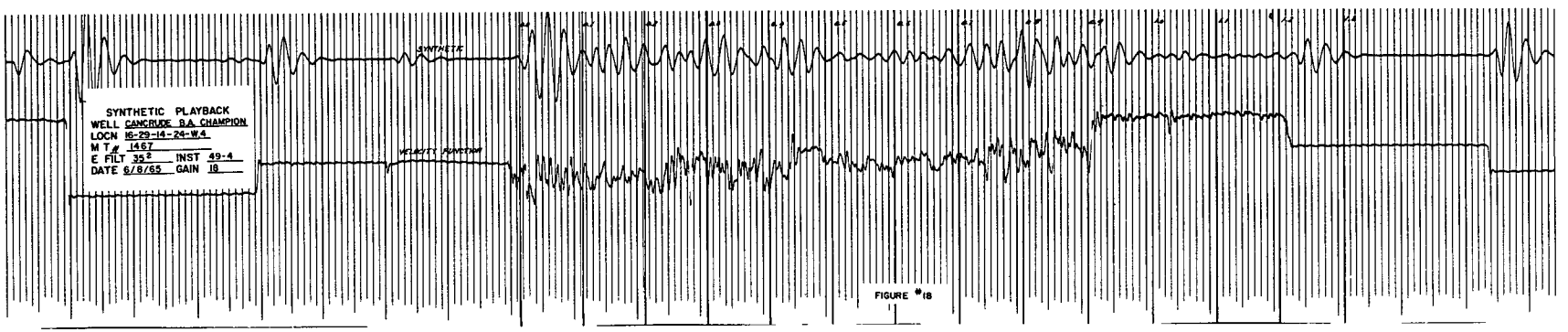

B.A. Cancrude Champion 16-29 synthetic playback

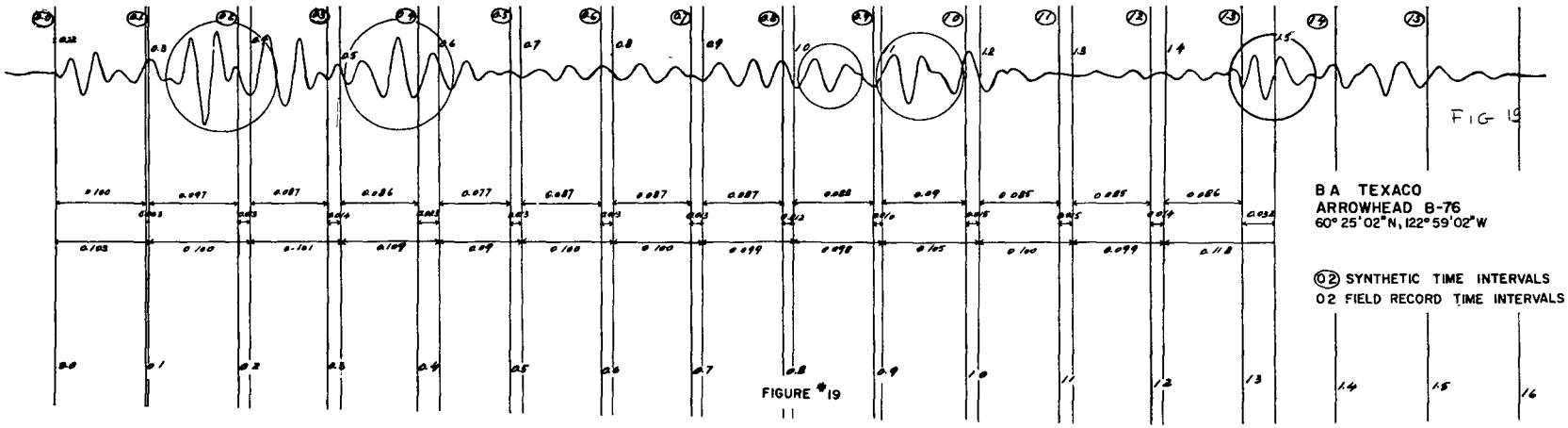

FIGURE #19

B.A. Texaco Arrowhead B-76 time discrepencies

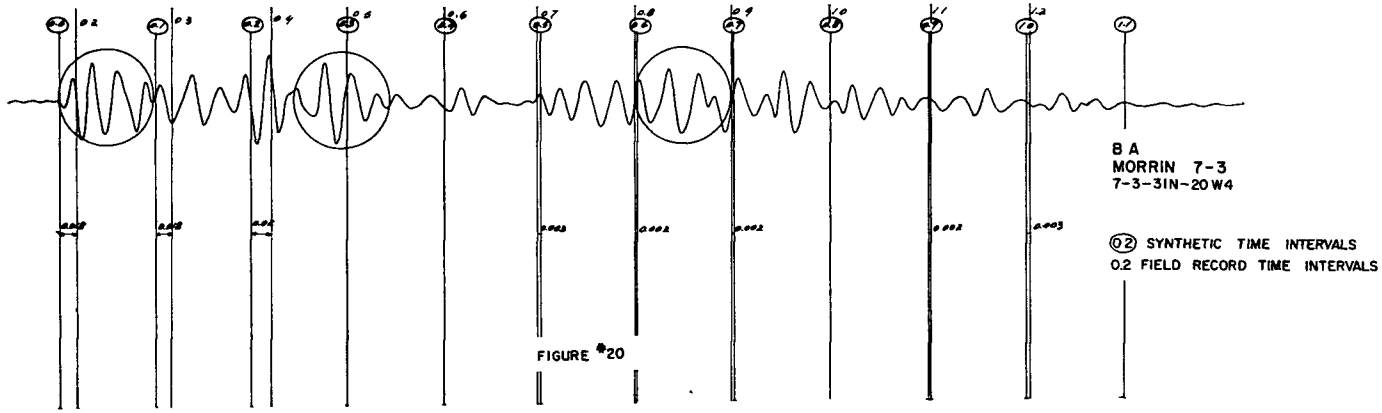

FIGURE #20

B.A. Morrin 7-3 time discrepencies

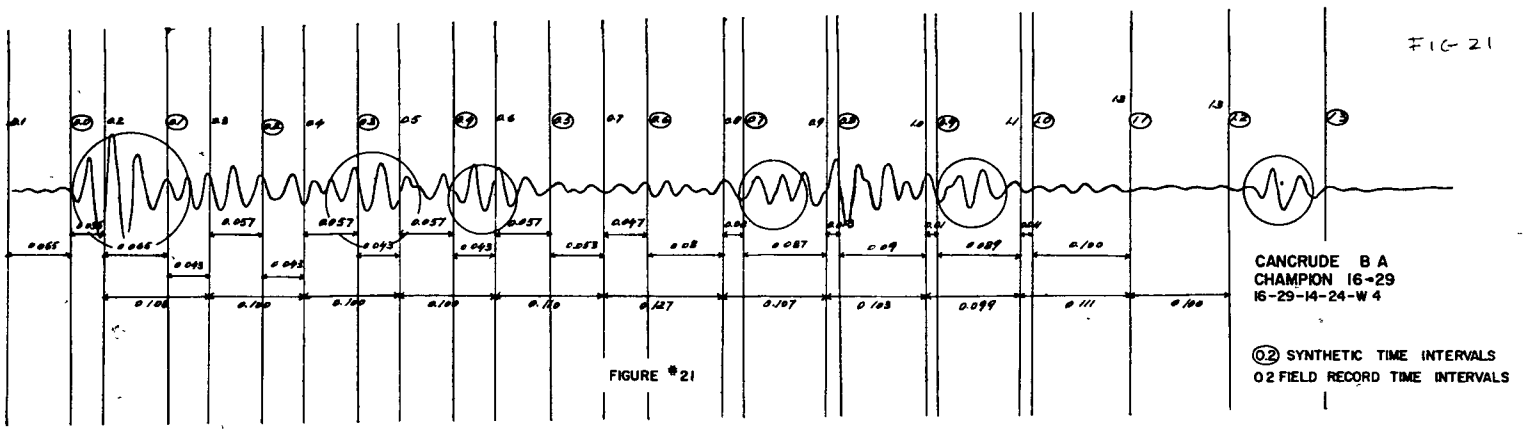

B.A. Cancrude Champion 16-29 time discrepencies

the best character match between synthetic and field records, the time intervals of the field record can be transferred to the synthetic record.

5. On the playouts of the function generator tapes, the time intervals for a hundred milliseconds are shown at the top of the graph (Figures 22, 23, 24). The depth intervals for each 1000 feet are also shown on the depth scale. Using the same time and depth intervals, a time-depth graph can be made (Figures 25, 26, 27). On this graph, depth is the ordinate and the two-way time is the abscissa. At the origin of this graph, time will be assumed zero and the depth will be starting depth value of the log. The time intervals can also be plotted on the depth scale, similarly assuming that the origin is zero time. In Figure 25, the straight line (A) passing through the origin, shows a two-way time-depth curve, assuming that the start of the velocity function is zero time. The second straight line (B), indicated by cross points, shows the actual two-way time-depth curve.

The actual two-way time-depth curve can be obtained in the following manner. First, the synthetic time intervals are plotted on the two-way time scale, taking into consideration the time differences between synthetic and field records. At this point it should be noted that the time interval on the synthetic record is not equal to the time interval on the velocity function which is shown at the top

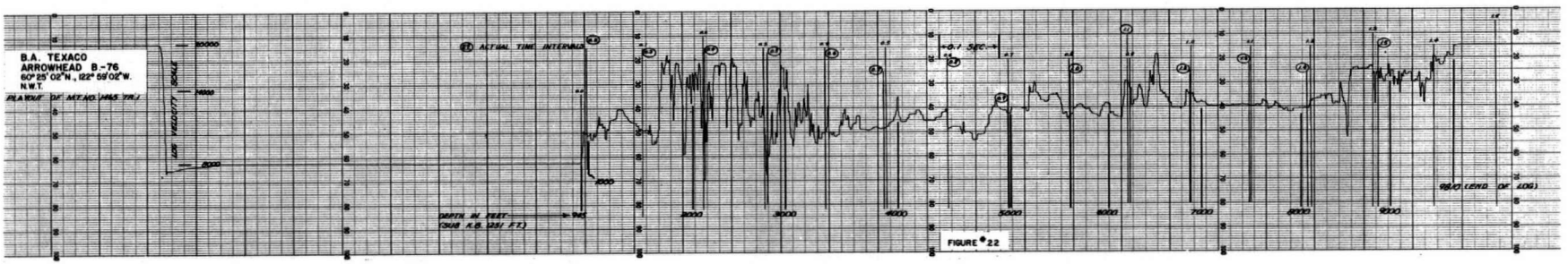

B.A. Texaco Arrowhead B-76 reflectivity function playout

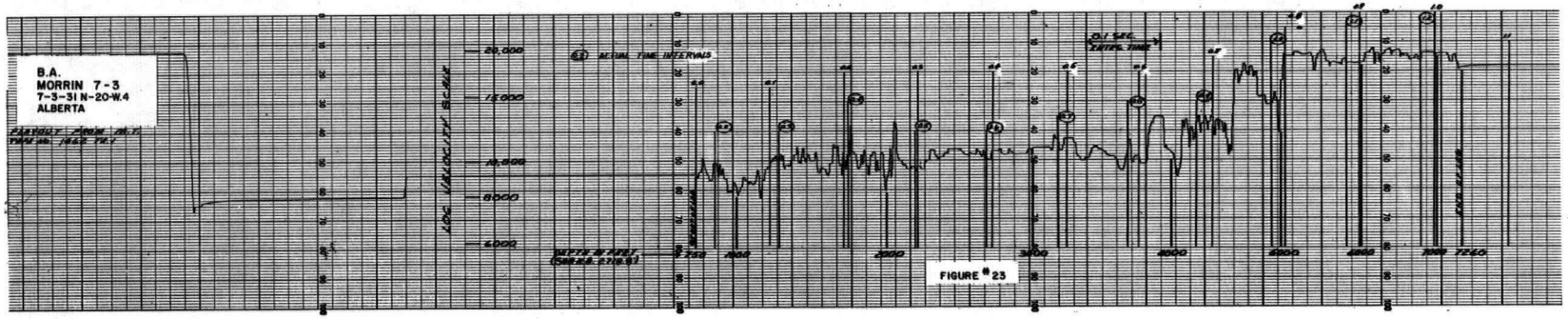

B.A. Morrin 7-3 reflectivity function playout

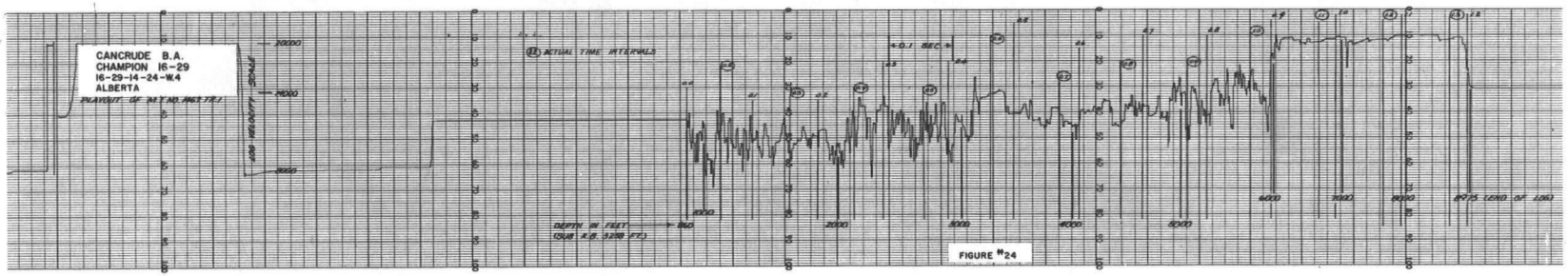

B.A. Cancrude Champion 16-29 reflectivity function playout

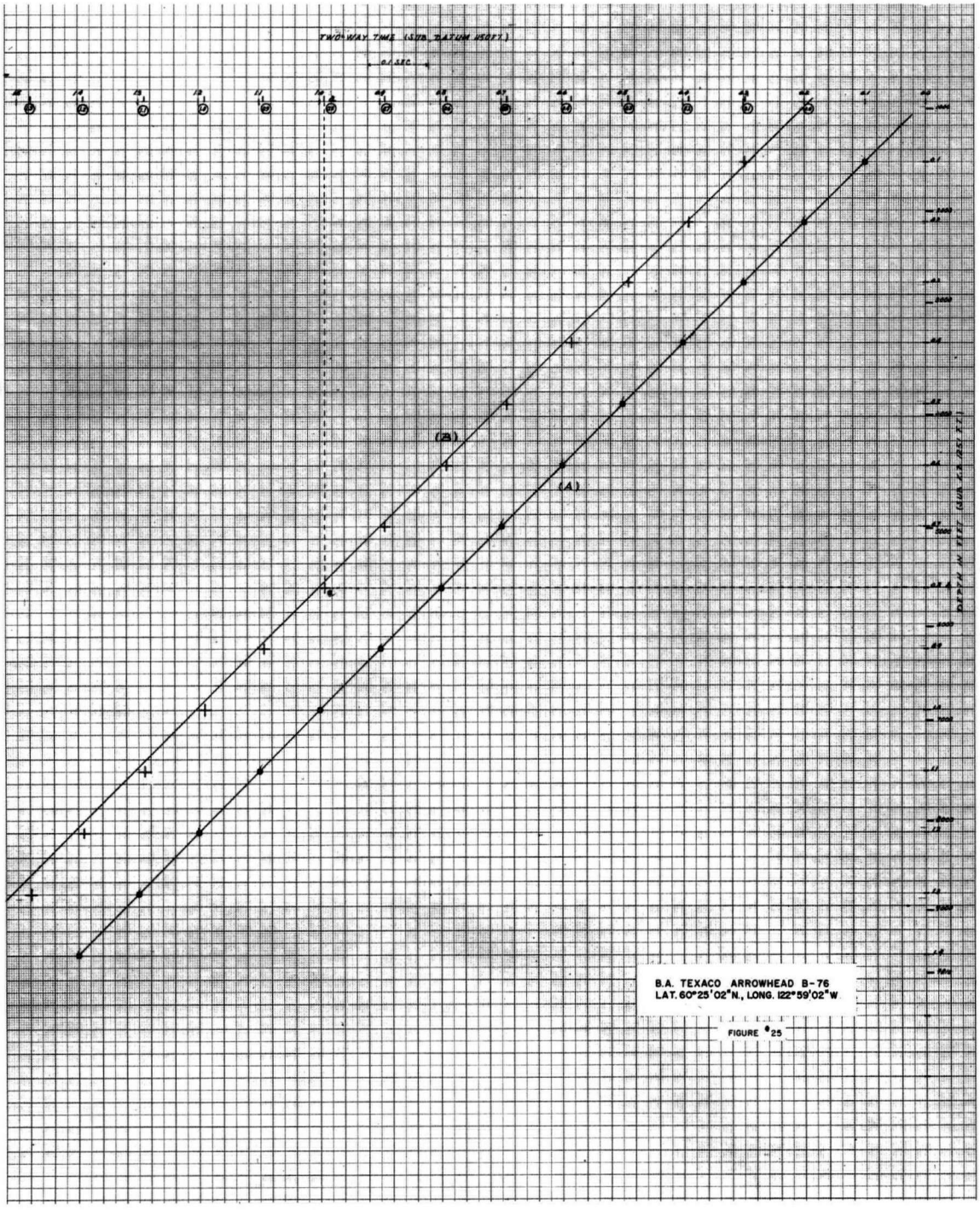

B.A. Cancrude Champion 16-29 two-way time-depth curve

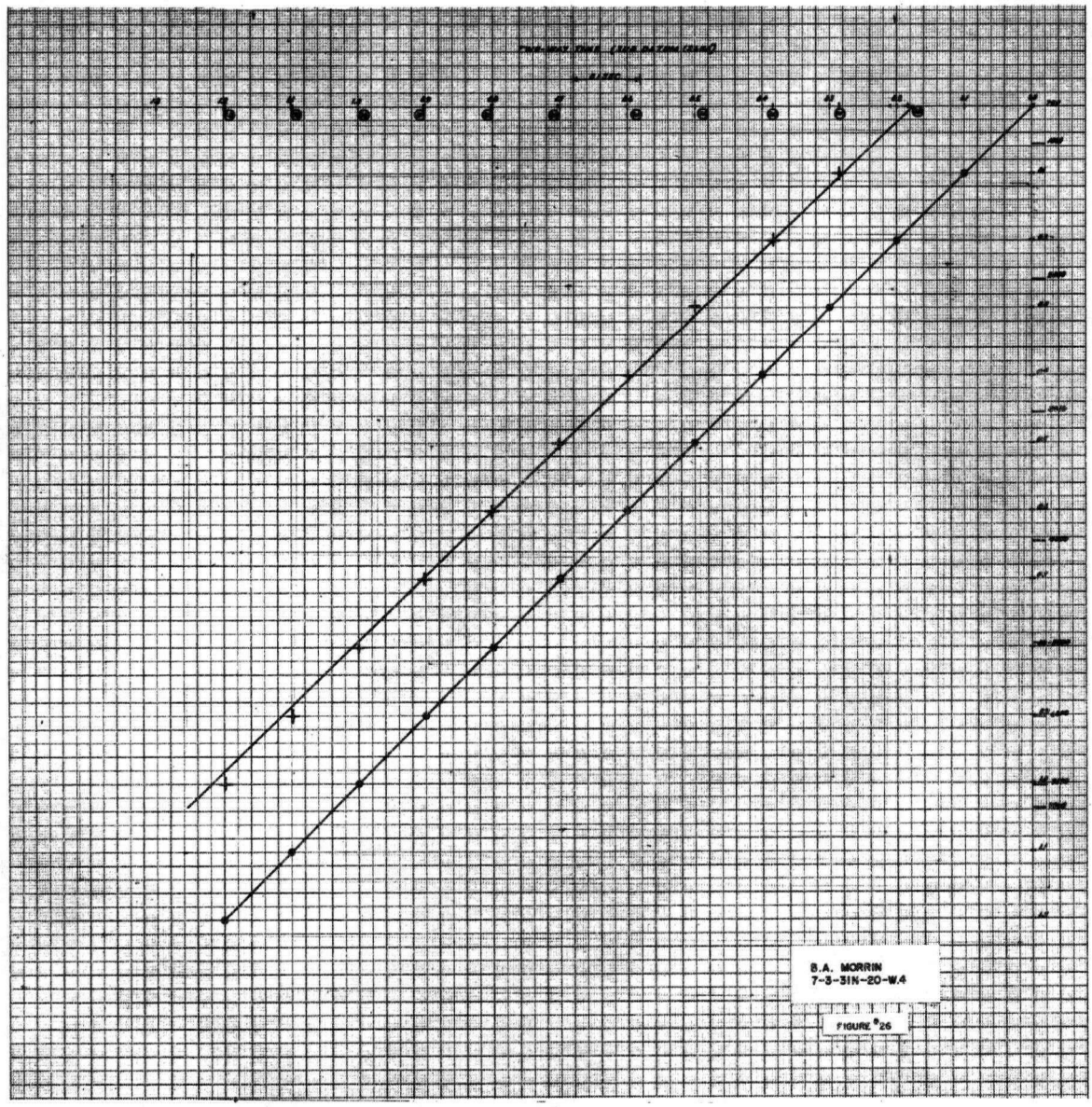

B.A. Morrin 7-3 two-way time-depth curve

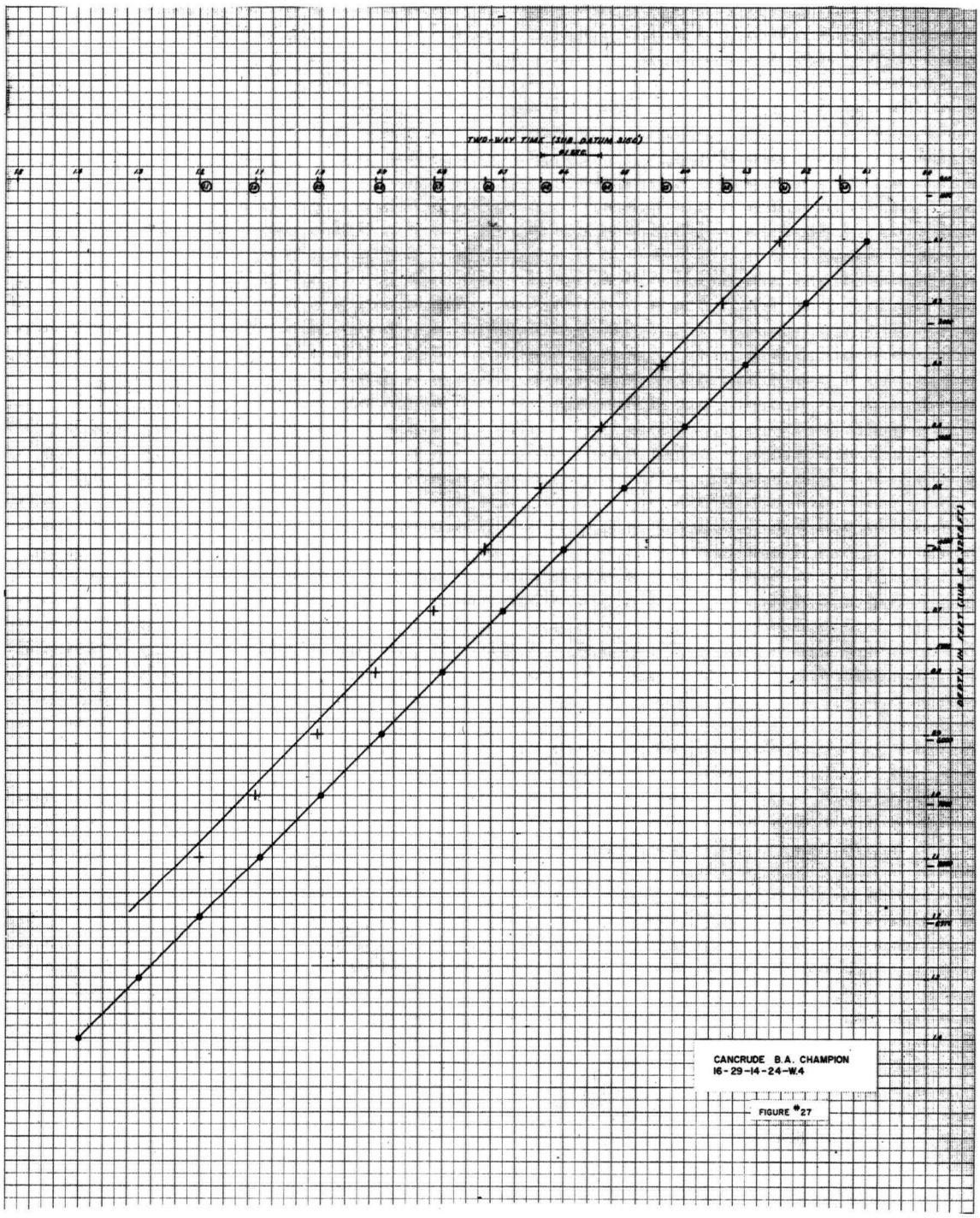

B.A. Texaco Arrowhead B-76 two-way time-depth curve

of the playouts of the function generator tapes (Figures 22, 23, 24). This discrepancy is four milliseconds. This matter should be considered before plotting the synthetic time interval points on the two-way time scale. Then, if these synthetic time interval points are extended vertically and the corresponding time intervals on the depth scale are extended horizontally, they will intersect at cross points. The straight line passing through these points will result in the actual two-way time-depth curve. To illustrate this point, let us consider the following example. In Figure 19 the time difference between the synthetic time (0.8 seconds) and the field time (1.0 seconds) is 0.012 seconds. As it can be seen in Figure 19, the field time according to the synthetic time is 0.012 seconds later in time; so that the exact place of the synthetic time on the two-way time scale (Figure 25) is 0.988 seconds (designated by a letter a). If this point is extended vertically and the corresponding time of 0.8 seconds (designated by a letter b) is extended horizontally, they will intersect at cross point c. The other cross points on this graph can be found in the same manner.

CHAPTER IV

RESULTS

4.1 Data

Using these steps, it was attempted to calibrate the continuous velocity logs. The studies were carried out at three different wells.

Following are the names and locations of these wells:

1. Texaco Arrowhead B-76
   60° 25' 02" N; 122° 59' 02" W
2. B.A. Morrin 7-3
   Lsd. 7, Section 3, Twp. 31N, Rge. 20, W4M
3. Cancrude B.A. Champion 16-29
   Lsd. 16, Section 29, Twp. 14, Rge. 24, W4M

The locations of the wells used in this work are shown in Figure 12.

The function generator tapes and their playouts are obtained from the uncalibrated continuous velocity logs of these three wells. From these function generator tapes, synthetic records were produced resulting in the best correlations with the field records.

The filters used in producing the synthetic records at these three wells were as follows:

			Slopes (in Db/oct. at %5 amp.)	
	LC (c.p.s.)	HC	LC (c.p.s.)	HC
(a) B.A. Texaco Arrowhead B-76				
Instrument Filter	22	62	16	22
Earth Filter	25	25		
(b) B.A. Morrin 7-3				
Instrument Filter	28	81	18	20
Earth Filter	25	25		
(c) B.A. Cancrude Champion 16-29				
Instrument Filter	28	81	18	20
Earth Filter	35	35		

The time interval lines are drawn on both records at every 100 milliseconds. Before setting the time intervals on the field records, the time corrections were made using the following data:

B.A. Texaco Arrowhead

Shot Point Elevation	=	1275'
Elevation Datum	=	1150'
Weathering Correction	=	0.014
Shot Hole Depth	=	40'
Elevation Correction Velocity	=	6000'/sec.
Total Time Correction	=	0.049 sec.

B.A. Morrin 7-3

Shot Point Elevation	=	2702'
Elevation Datum	=	2650'
Weathering Correction	=	0.0273
Shot Hole Depth	=	70'
Elevation Correction Velocity	=	6500'/sec.
Total Time Correction	=	0.027915 sec.

Cancrude B.A. Chamption 16-29

Shot Point Elevation	=	3243'
Elevation Datum	=	3150'
Weathering Correction	=	0.018
Shot Hole Depth	=	71'
Elevation Correction Velocity	=	11000'/sec.
Total Time Correction	=	0.032

Then the synthetic and field records are correlated (Figures 19, 20, 21). The time difference between synthetic and field record time intervals are in the range of 0.01 - 0.065 sec. at Cancrude B.A. Champion, from 0.002 seconds to 0.02 seconds at B.A. Morrin, and between 0.003 and 0.032 seconds at B.A. Texaco Arrowhead.

As a final step, the two-way time-depth curves were plotted for these three wells (Figures 25, 26, 27). From these curves the time intervals of continuous velocity logs were determined to be in error by $\pm$ 0.007 seconds to $\pm$ 0.00825 seconds.

In tables 1 to 3, the velocity analysis data at these three wells are tabulated. The results of this study can be checked with the values shown in these tables.

4.2 The Discussions of the Errors in Time Scale of Synthetic Seismograms

Over a period of time, non uniformity of timing lines for synthetic seismograms has been recognized as a symptom of error, with questions as to the nature of such

LOCATION N60°25'02"W122°59'02"

WELL NAME B.A. TEXACO ARROWHEAD B-76

AREA FT. SIMPSON

K B. 1265

G.L. 1250

GEOLOGIC FORMATION	DEPTH FROM K.B	ELEVATION FT FROM SEA LEVEL	REFLECTION TIME SECS (TWO-WAY)
SCATTER	1078	173	.218
L.BUCKINGHORSE	1175	76	.2390
FLETT.	1607	-356	.326
BNFF.	3258	-2007	.576
EX.	4817	-3566	.872
KOTCHO	4862	-3611	.882
F. LIME	5185	-3934	.924
TETCHO	6105	-4854	1.086
TROUT RIVER	6215	-4964	1.1032
KAKISA	6482	-5232	1.142
RED KNIFE FORT SIMSON	6548	-5297	1.149
MUSKWA	8448	-7197	1.4586
SLAVE POINT	8479	-7228	1.464
WATT	8790	-7539	1.492
PINE PT. DOLOMITE	8823	-7572	1.4923
T.D.	9805	-8554	1.59

TABLE #1

LOCATION 7-3-31-20 W.4

WELL NAME B.A. MORRIN

AREA MORRIN

K B 2719

G L. 2705

GEOLOGIC FORMATION	DEPTH FROM K B	ELEVATION FT FROM SEA LEVEL	REFLECTION TIME SECS (TWO-WAY)
L.P.	2060	659	.472
COLO.	2553	166	.5666
2 WS	3420	-701	.744
B.F.S.	3696	-977	.802
VIK.	3814	-1095	.82
MANV.	4072	-1350	.87
GLAUC.			
PEK.	4498	-1779	.946
BNFF.	4676	-1957	.964
EX.	4970	-2251	1.0073
WAB.	4985	-2266	1.008
STET.	5018	-2299	1.012
CAL.	5495	-2776	1.062
NIS.	5506	-2787	1.064
NIS. POR.			
IRE.	5651	-2932	1.0802
LED.	5688	-2969	1.0856
DUV. EQUIN.			
CK. L.	6390	-3671	1.16
B.H.L	6600	-3881	1.1816
EP.	7202	-4483	1.2430
T.D.	7264	-4545	1.248

TABLE #2

LOCATION 16-29-14-24-W.4

WELL NAME CANCRUDE B.A. CHAMPION

AREA CHAMPION

K B 3256

G L. 3243.3

GEOLOGIC FORMATION	DEPTH FROM K B	ELEVATION FT FROM SEA LEVEL	REFLECTION TIME SECS (TWO-WAY)
B.P.	1378	1878	.243
B.R.	1950	1306	.362
PAK.	2933	323	.544
MR.	3082	174	.5710
COLO.	3471	-215	.6302
2WS.	4479	-1223	.803
BFS.	4802	-1546	.855
B. IS.	4862	-1606	.865
BL.	5278	-2022	.931
OST.	5693	-2437	.992
BSL. QTZ.	5748	-2492	.9996
SWIFT.	5780	-2524	1.004
RIER.	5808	-2552	1.0084
TV. UPOR.	5906	-2650	1.023
M. DENSE	5958	-2702	1.028
L.POR.	6002	-2746	1.0322
SHUNDA	6216	-2960	1.054
PEK.	6296	-3040	1.061
BNFF.	6496	-3240	1.0824
EX.	7072	-3816	1.141
WAB.	7082	-3826	1.142
FAIR.	7590	-4334	1.194
CK. L.	8283	-5027	1.261
B.H.L.	8467	-5211	1.2796
EP.	8877	-5621	1.321
CAMB.	8896	-5640	1.3232
T.D.	8973	-5717	

TABLE #3

error being raised in consequence. In large degree, any errors are directly related to error in the basic velocity log and analysis thereof.

The starting point of the reflectivity function is arbitarily chosen as zero time and 100 milliseconds are placed on the record. (See Figures 22, 23, 24.) It is clear that the time differences between these timing lines and the actual timing lines should be the same. But it can be seen from these figures (22, 23, 24) that differences change irregularly throughout the record.

We have concluded that accuracy limitations inherent in integrating equipment and its operation result in discrepancies and that there are human errors in treating the data. More specifically, the basic limitations are:

1. Field and laboratory systems as operated integrate and display data with limited fidelity. One consequence is that the integration of the velocity log carried out at magnetic tape function generator sometimes differs from the field integration. The integration systems at magnetic tape function generator has an accuracy under normal operating conditions of $\pm$ 1% and presumably the field integration systems have a similar accuracy.

Velocity logs presented with only velocity scale involve and require additional processing with consequent unavoidable degradation accuracy. These limitations are intrinsic in the synthetic seismograms produced from the

logs and are in part instrumental and in part human.

The comparatively minor source of non uniformity subject to correction is:

2. Entirely human error in drafting and presentation including improper transfer of times from the calibrated linear depth log to the new linear time log.

The differences between field and magnetic tape function generator integrations is a most important source of discrepancies. In producing a synthetic seismogram, the linear depth vertical scale of the calibrated velocity log is converted to a linear time vertical scale. This operation requires an integration of the calibrated log. The problem is to maintain correct association of integrated times with the appropriate discrete velocity measurements. If the new integration repeats the corrected field integration (i.e., if the association of velocity measurements with integrated times on the new linear time log duplicates the association of velocity measurements at these same times on the calibrated linear depth log), equal time intervals will in fact be linearly spaced on the linear time log. However, a disagreement between the two integrations will be evidenced by the fact that timing lines on the laboratory integrated linear time log will be associated with different velocity measurements than those appearing at these same times on the calibrated linear depth field log. As the field integration is computed directly in logging device, whereas magnetic tape function generator integration derives from additional curve plotting

and tracing steps, the association of vertical integrated times and discrete velocity measurements on the calibrated field log is adopted. As a result, the time intervals transferred from the calibrated field log onto the linear time log will generally not be of the same length. The lack of fidelity or malfunction of field integrating equipment or handling requires one to recalibrate the log.

The second source of the discrepancies is due to time-to-linear velocity conversion of horizontal scale. This type is peculiar to velocity logs which are only with a linear velocity horizontal scale instead of the more basic linear time horizontal scale. The integration of these logs can be done by reconverting from a linear velocity scale to a linear time scale. After this, normal integration processes are used. Consequently, the log has two additional times.

Such integrations, when completed, commonly differ from the calibration times and often appreciably. In practice, it is felt that these additional conversion processes, from linear time to linear velocity and then back from linear velocity to linear time, compound the discrepancies. It is postulated that the reason for this is difficulty in obtaining linearity in the electrical circuit simulating the conversion.

4.3 Interpretation of Results:

a. B.A. Texaco Arrowhead

The well was started in Buckinghorse formation at 1078 ft. and bottomed in Pine Point Dolomite at approximately 8800 ft. The synthetic records are compared with a field record taken near the well. The object of this comparison will be to determine which synthetic record more closely resembles the reflected signal on the field record. The synthetic record which agrees most closely with the reflection record shows the best correspondence at times near 0.37 sec., 0.58 sec. and 1.13 sec. (as shown in circles in Figure 19). The field record shows that a multiple comes from the first reflection at 1.5-1.6 sec. The high velocity distribution occurs between 0.3-0.5 sec. The oscillations on the synthetic record vary quite smoothly as though the entire record has been played through a very narrow band filter.

b. B.A. Morrin

The continuous velocity log covered the depth range from approximately 800 ft. to 7200 ft. A correspondence between the synthetic and the field records shows that there are agreements at times 0.45, 0.6, 0.85-0.95 sec.

There is interference at 0.8-0.9 sec. which comes from the first reflection event. The synthetic record has been time shifted approximately 0.5 m.s. to the right to establish the correspondence between high velocity zones and peaks on the field record. The main events

visible on the seismic record are:

(a) weaker reflections from deeper horizons and

(b) very little interference or noise. The oscillations on the synthetic record show rapid changes of amplitude.

c. B.A. Concrude Champion:

The continuous velocity log was recorded between 877 ft. and 8973 ft. The strong reflection events on the field record are matched with the synthetic record at 0.57-0.9 and 1.05 sec. The synthetic record has the same polarity as the field record, as determined from the initial down break of the reflection from the artifical step placed near the beginning of each velocity function. The reflectivity function shows much smaller velocity contrasts than that of the previous two examples. The synthetic record has been displaced about 4 milliseconds to match the strong reflection events.

The correlation of synthetic records with field records at different locations is shown in Figures 28 and 33.

The synthetic records in each case have the same polarity as the field record. The polarity is determined from the initial break of the reflection from the artificial step placed near the beginning of each reflectivity function. (See Figures 16, 17, 18.) This fulfills the third criterion for good match.

The synthetic and field records in Figures 28 and 33 are displaced with zero relative time shift, in accordance with the second criterion. The wide peaks correspond to "thick" bed or velocity zones and narrow peaks correspond to "thin" bed zones.

Figures 28, 29 and 30 are chosen as examples of velocity distributions for which multiples are not significant. In these examples the interfaces are smooth and parallel. The records show that seismic energy is received in appreciable amounts at all times after the transmission of the incident pulse. The large amplitude oscillations are as apt to be the result of constructive interference as of prominent individual contrasts. It can be seen (Figure 28) that the largest amount of incident energy does not necessarily produce the highest amplitude oscillations on the record. The amplitude of the oscillation at 0.84 seconds is less than that at 1.12 seconds despite the fact that the incident energy is greater than at 0.82 seconds.

Figures 31, 32 and 33 are examples wherein multiples are important throughout the duration of the reflected signal. The prominent multiples are designated by letter 'M'. The multiples caused considerable phase shift in the direct reflected signal. The differences between the synthetic and field record are rather small especially at the earlier arrival times. (Figures 31, 32.) At later times the two records appear to become appreciably

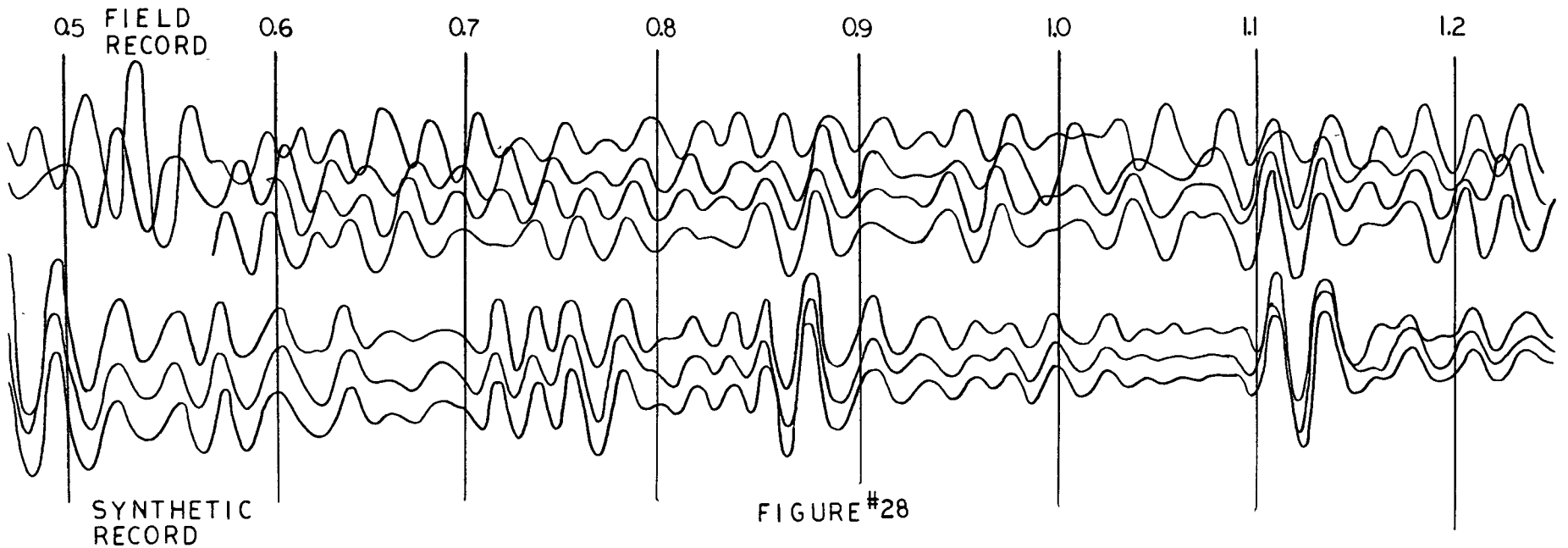

Comparision of field record with synthetic record

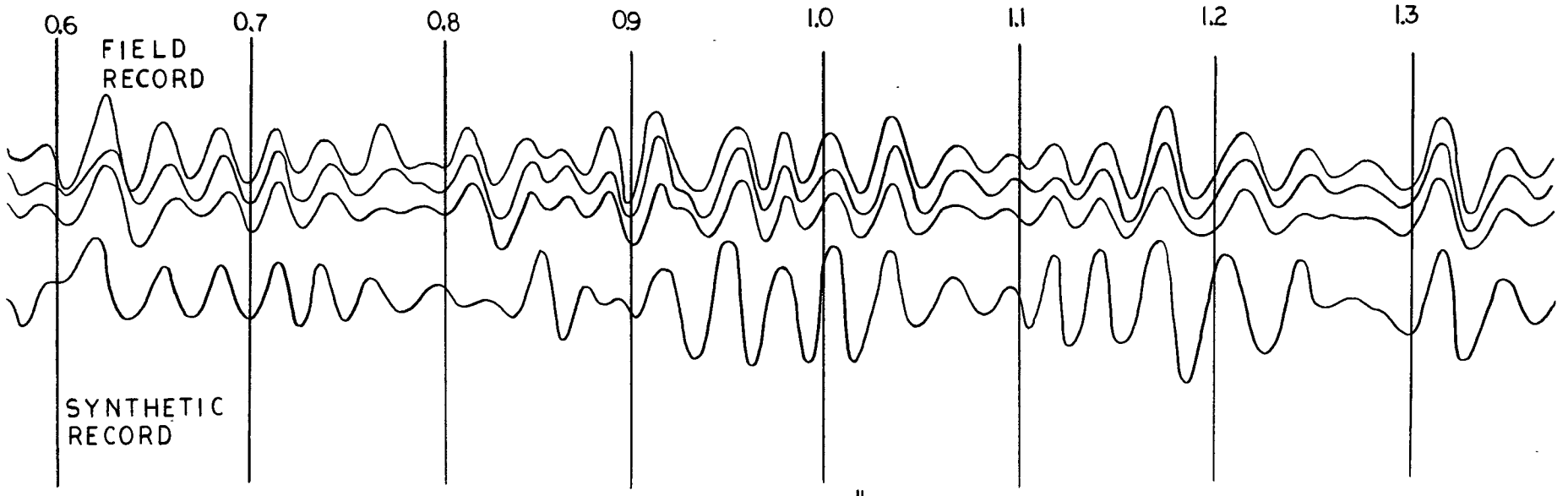

FIGURE # 29

Comparision of field record with synthetic record

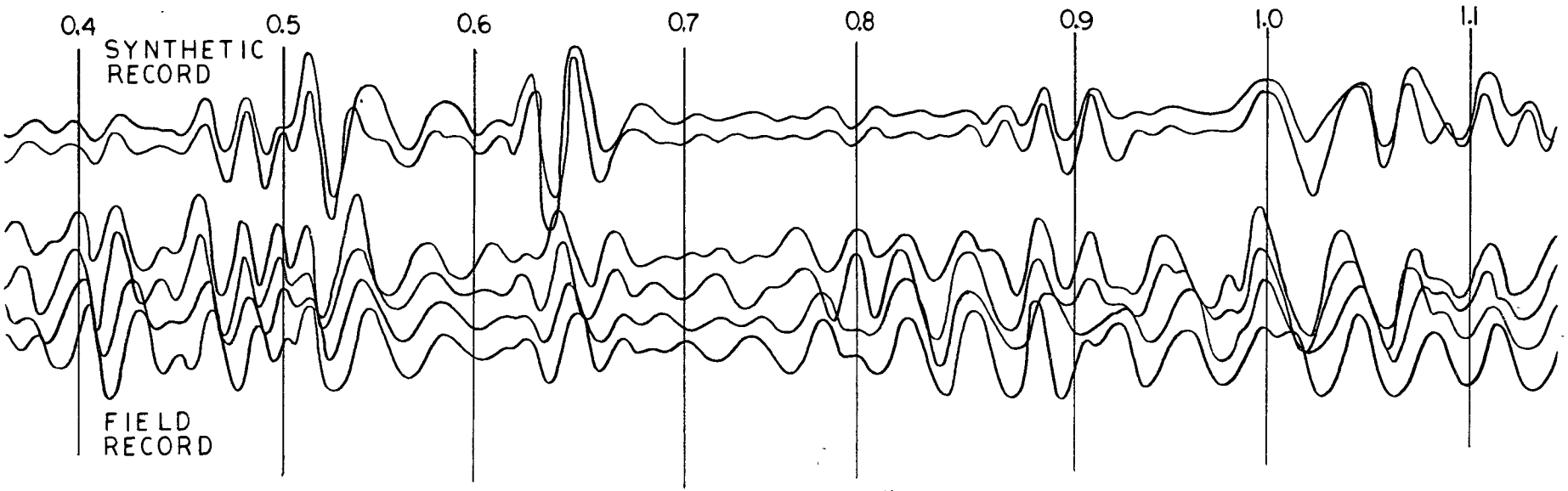

FIGURE # 30

Comparision of field record with synthetic record

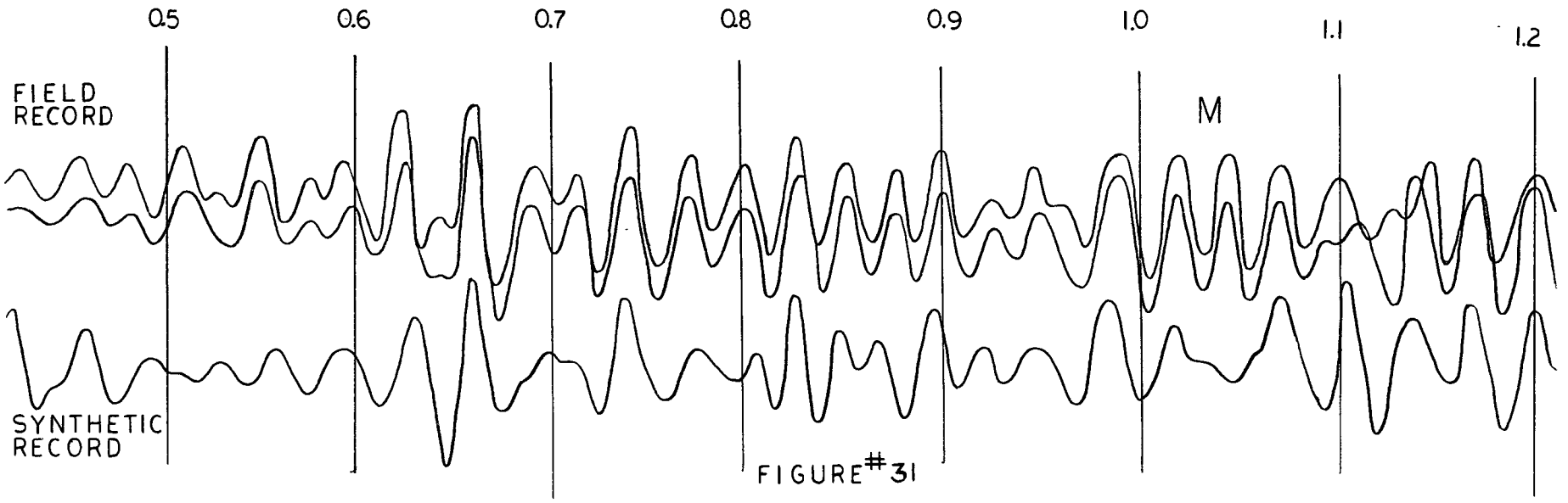

Comparision of field record with synthetic record

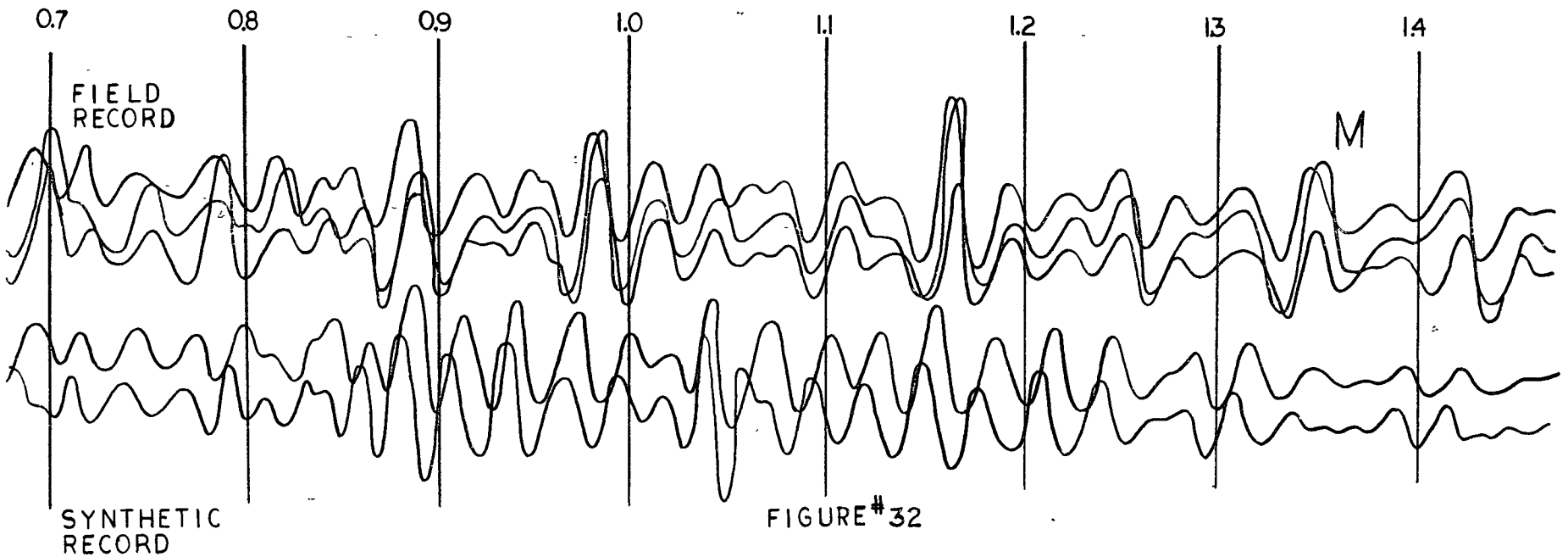

Comparision of field record with synthetic record

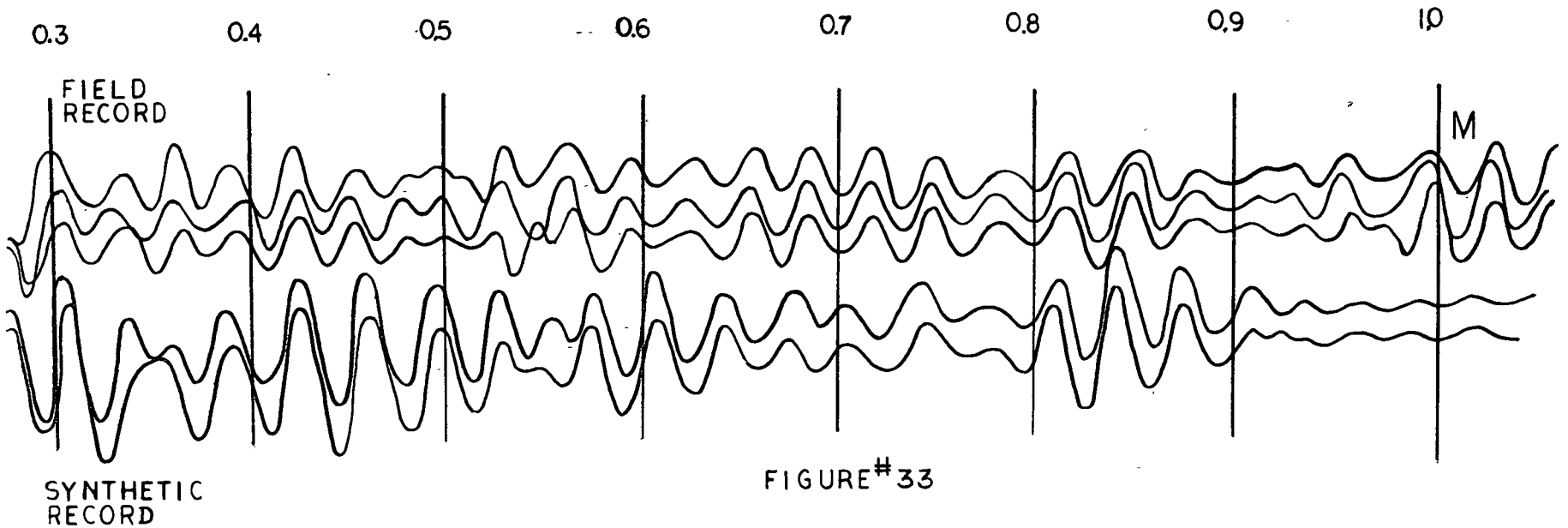

FIGURE # 33

Comparision of field record with synthetic record

different. If the phase shift due to the multiples which causes this apparent lack of similarity is removed, the correlation will be improved. A third example (Figure 33) shows a pair of multiples reflection. The records appear very similar, but the subtraction of one from the other shows that phase shift is causing an increasing divergence at later times.

CHAPTER V

CONCLUSION

In this study, only a limited number of synthetics have been prepared for comparison with actual field records obtained at the corresponding well locations. The results of this study proved that there is a possibility of calibrating continuous velocity logs using the comparison of synthetic and field records. During this research the best correlations were obtained at thirteen different locations. In some cases, poor correlations were obtained in spite of the good quality of the reflection record. This poor agreement may be partially explained by the fact that the synthetic seismogram produced by Peterson's method only approximates the true reflected signal. An improvement in obtaining a "good match" would be expected if the approximation used by Peterson could be avoided. Peterson's technique consists of neglecting transmission coefficients, multiples and ghost reflections, and assuming that the density is constant. He further finds approximations for the reflection coefficients at each change in acoustic impedance using one half the fractional difference of the velocity across the contrasts. The mathematical approximation will more closely approach ideal situations by including multiples and transmission coefficients. Further improvement can be obtained by computing exactly the reflected signal of plane waves incident normal to the surface of a multilayered half space, in the case where

the source is a unit impulse in time.

It was found that the following factors must be taken into account in the calibration of continuous velocity logs using this procedure.

1. When making the time correction for weathering and elevation variations, the elevation datum of the well data should be used for the actual seismic record.
2. The correlation between the synthetic and field records should be made between strong reflection events.
3. It was found that the time interval on the synthetic record is not equal to the time interval on the velocity function playout. Therefore, the time interval of the synthetic record should be converted to the time interval of velocity function before plotting the synthetic time intervals on the two-way time depth graphs.
4. A correspondence should be established between the synthetic record and the velocity function by shifting the synthetic forward in time.
5. Any significant move-out on the seismic record should be removed before comparison with the synthetic record.

BIBLIOGRAPHY

Austey, N. A., Correlation Techniques, A Review By, Seismograph Service Corporation, Tulsa, Oklahoma.

Backus, M. M., Water Reverberations, Their Nature and Elimination, Geophysics, Vol. 24, 233-261, 1959.

Berryman, L. H., P. L. Goupillaud and K. H. Weters, Reflection From Multiple Transition Layers, Part I, Therical Results, Geophysics, Vol. 23, 223-243, 1958.

Birch, F., and Bancroft, Elasticity and Internal Friction in a Long Column of Granite, Bull. Seis. Soc. Amer., Vol. 23.

Bruckshaw, J. M., and P. C. Mahanta, The Variation of the Elastic Contents of Rocks with Frequency, Mimeographed Circular of the E.A.E.G., 1952.

Cholet, J., and H. Richard, A Test on Elastic Anisotropy Measurements at Berriane (North Sahara), Geophys. Prospecting, Vol. 2, No. 3, 1954.

Delaplanche, J., An Example of the use of Synthetic Seismograms, Geol., Vol. 28, No. 5, 843, 1963.

Dunoyer de Segonzac, P., and Loherrere, Application of the Continuous Velocity to Anisotropy Measurements in Northern Sahara, Results and Consequences, Geophys. Prospecting, Vol. 7, No. 2.

Gretener, P. E. F., An Analysis of the Observed Time Discrepancies Between Continuous and Conventional Well Velocity Surveys, J. Alberta Soc. Petro. Geologists, Vol. 8, No. 10, 272-286, 1960.

Hicks, W. G., Lateral Velocity Variations Near Boreholes, Geophysics, Vol. 24, No. 3, 451-464, 1959.

Kokesh, F. P., and R. B. Blizard, Geometrical Factors in Sonic Logging, Geophysics, Vol. 24, No. 1, 64-76, 1959.

Lindsey, J. P., Elimination of Seismic Ghost Reflections by Means of Linear Filter, Geol. Vol. 25, No. 1, 130-140, 1960.

Lee, Y. W., Statistical Theory of Communication, New York, London, John Wiley and Sons Inc.

Peterson, R. A., W. R. Fillippone, F. B. Coker, The Synthesis of Seismograms from Well Log Data, Geophysics, Vol. 20, No. 3, 516-538, 1955.

Richards, T. C., Wide-Angle Reflections and Their Application to Finding Limestone Structures in the Foothills of Western Canada, Geophysics, Vol. 25, No. 2, 385-407, 1960.

Ricker, N., Wavelet Contraction, Wavelet Expansion and the Control of Seismic Resolution, Geophysics, Vol. 18, No. 4, 769-792, 1953.

Ricker, N., The Form and Lows of Propagation of Seismic Wavelets, Geophysics, Vol. 18, No. 1, 11-40, 1953.

Ricker, N., The Form and Nature of Seismic Waves and the Structure of Seismograms, Geol., Vol. 5, No. 4, 349-366, 1940.

Sengbush, R. L., P. L. Lawrence, and F. J. McDonal, Interpretation of Synthetic Seismograms, Geophysics, Vol. 26, No. 2, 138-156, 1961.

Summers, G. C., and R. A. Broding, Continuous Velocity Logging, Geophysics, Vol. 17, No. 3, 598-614, 1952.

Smith, M. K., A Review of Methods of Filtering Seismic Data, Geophysics, Vol. 23, No. 1, 44-57, 1958.

Vogel, C. B., A Seismic Velocity Logging Method, Geophysics, Vol. 17, No. 3, 587-597, 1952.

White, J. E., Seismic Waves Radiation, Transmission and Attenuation, McGraw Hill.

Wolf, A., The Time Delay of a Wave Group in the Weathered Layer, Geophysics, Vol. 5, 367-372, 1940.

Wolf, A., The Reflection of Elastic Waves From Transition Layers of Variable Velocity, Geophysics, Vol. 2, 357-363, 1937.

Woods, J. P., The Composition of Reflection, Geophysics, Vol. 21, No. 2, 261-276, 1956.

Wuenschel, P. C., Seismogram Synthesis Including Multiples and Transmission Coefficients, Geophysics, Vol. 25, No. 1, 106-129, 1960.

Wyllie, M. R. J., A. R. Gregory, and G. H. F. Gardner, An Experimental Investigation of Factors Affecting Elastic Wave Velocities in Porous Media, Geophysics, Vol. 23, No. 3, 459-493, 1958.